STRUCTURAL OPTIMIZATION FOR CONTROL OF STIFFENED LAMINATED COMPOSITE PLATES, USING NONLINEAR MIXED INTEGER PROGRAMMING

by

Luis Clemente Mesquita

Dissertation submitted to the Faculty of the
Virginia Polytechnic Institute and State University
in partial fulfillment of the requirements for
the degree of

DOCTOR OF PHILOSOPHY

in

ENGINEERING MECHANICS

APPROVED:

Manchar P. Kamat, Chairman

Raphael T. Haftka

Mahendra P. Singh

Leonard Meirovitch

William L. Hallauer

July 1985
Blacksburg, Virginia

STRUCTURAL OPTIMIZATION FOR CONTROL OF STIFFENED LAMINATED COMPOSITE PLATES USING NONLINEAR MIXED INTEGER PROGRAMMING

by

Luis Clemente Mesquita

Dissertation submitted to the Faculty of the
Virginia Polytechnic Institute and State University
in partial fulfillment of the requirements for
the degree of

DOCTOR OF PHILOSOPHY

in

ENGINEERING MECHANICS

(ABSTRACT)

The effect of structural optimization on control of stiffened laminated composite structures is considered. The structural optimization considered here, is the maximization of structural frequencies of the structure subject to maximum weight and frequency separation constraints and an upper bound on weight. The number of plies with a given orientation and the stiffener areas form the two sets of design variables. As the number of plies is restricted to integer values, the optimization problem considered belongs to the class of nonlinear mixed integer problems (NMIP). Several efficiency measures are proposed to reduce the computational cost for solution of the optimization problem. Savings in computer time due to each of the measures is discussed. The control problem is solved using the independent modal space control technique. This technique greatly simplifies the evaluation of the sensitivity of the performance index with respect to the individual frequencies.

The effect of different optimization schemes on the control performance is considered. To reduce the probability, that conclusions drawn from numerical results, are purely coincidental, a large number of cases has been studied. It has been concluded that sufficient improvement in control performance can be achieved through structural optimization.

ACKNOWLEDGEMENTS

The author wishes to express his sincere gratitude to his advisor Dr. Manohar P. Kamat for the enthusiasm, assistance, guidance and suggestions which made the completion of this work possible. His reviewing and correcting the manuscript is also appreciated.

The author sincerely expresses his gratitude to Dr. Raphael T. Haftka, Dr. William L. Hallauer, Dr. Leonard Meirovitch and Mahendra P. Singh for serving on the Advisory Committee.

The author wishes to thank the Engineering Science and Mechanics Department for providing Graduate Assistantship during the duration of this work. This work was also supported by U.S. Air Force under Contract #F33615-83/k-3214. Dr. V. B. Venkayya was the responsible contract monitor.

Most of the computational work was done on Computer Science department VAX 11/780 and the use of this facility is greatly appreciated. Special thanks are due to Dr. Layne T. Watson, who made the use of this facility possible.

He wishes to thank for typing the manuscript. Her patience in typing the numerous equations in this text is appreciated.

The author would like to take this opportunity to thank his colleagues and friends in Blacksburg. Last but not least, the author would like to thank his parents, sisters and brothers for their moral support.

LIST OF SYMBOLS

a_i	Nondimensional area of the i^{th} stiffener.
A	Dimensional area in unspecified but consistent units for the stiffeners.
	Open loop plant matrix.
	Laminate stiffness matrix for inplane loading.
	Hessian matrix for the Lagrangian function.
A_o	Reference area.
[b]	Largest integer value not exceeding b.
B	Actuator placement transformation matrix.
C	Control cost.
D	Laminate stiffness matrix for out of plane bending.
E_1, E_2, E_3	The Young's moduli in 1, 2 and 3 directions respectively.
f	Objective function in an optimization problem.
F	Nodal force vector.
E_p	Reduced order force vector with p actuators.
G	Gain matrix for feedback gains (Riccati matrix).
G_{23}, G_{31}, G_{12}	The shear moduli in the 2-3, 3-1 and 1-2 planes respectively.
g_i	Inequality constraint vector ($G > 0$).
h_i	Equality constraint vector.
H	Positive definite weighting matrix.
I_k	Moment of inertia of k^{th} element.
I_o	Reference moment of inertia.
J	Performance index (cost).
J_r	Performance index (cost) for the r^{th} mode.

LIST OF SYMBOLS CONTINUED

k,k	Shear correction factors.
K	System stiffness matrix.
M	System mass matrix.
m_i	Weighting factors.
n	Number of degrees of freedom of the finite element model.
n_e	Number of equality constraints.
n_g	Number of inequality constraints
n_i	Number of plies having orientation θ_i
p	Number of controlled modes.
Q	Positive definite weighting matrix.
	Prescribed frequency ratios.
R	Penalty parameter.
R_r	Penalty parameter for the r^{th} mode.
S	Search direction.
T	CPU time in seconds for a given subproblem
T_o	CPU time for the first continuous solution.
t	Thickness of individual plies.
t_f	Final time.
t_f	Initial time.
u	Generalized nodal displacement vector.
U_i	i^{th} eigenvector
w	Out of plane displacement along the Z axis.
v	State vector.
X	Modal matrix of eigenvectors.

LIST OF SYMBOLS CONTINUED

x	Design variable vector.
z_i	Height of the i^{th} ply as measured from the laminate mid-plane.
z_c	Modal control force vector.
β_i	Target for the i^{th} structural eigenvalue.
η	Modal space velocity.
λ_i	i^{th} structural frequency.
λ_{0i}	i^{th} structural frequency of the initial structure.
ν_{ij}	Poisson's ratio for transverse strain in the j-direction when stressed in the i-direction.
ω	Circular frequency in radians per second.
ρ	Density (mass per unit volume).
ψ_x	Shear rotation about the Y-axis (+ve clockwise).
ψ_y	Shear rotation about the X-axis (+ve clockwise).
θ_i	Orientation of the i^{th} ply in radians.
ξ	Modal space displacement.
	Local coordinate for plate elements.

TABLE OF CONTENTS

TABLE OF CONTENTS CONTINUED

LIST OF TABLES

LIST OF FIGURES

CHAPTER 1

INTRODUCTION

Structural optimization and control have been important research topics in the last two decades. Increased space applications have made such studies imperative, while the advent of fast computers has made these efforts feasible.

The objectives considered in structural optimization are usually

a) Minimization of structural mass

b) Minimization of maximum structural deflection or its appropriate norm, or

c) Maximization of fundamental frequency (or buckling load).

A combination of constraints on the stresses, deflections, frequency ratios, overall weight, member sizes etc. may be additionally imposed.

In structural control one of the aims is to damp out the motion resulting from some arbitrary excitation of the structure. Various sources of excitation are possible including electrical machinery, space maneuvers such as docking, etc. The motion resulting from this arbitrary excitation needs to be dampened, and this can be done in several ways.

In active control, the position and velocities of the structure at various points are measured and suitable control forces then applied. The designer selects a performance index and the control forces are applied in such a way that the performance index is minimized. The performance index, as the name suggests is a measure of how efficiently the controlling device performs its task.

Generally, in solving the control problem one does not modify the structure to be controlled. This is a somewhat restrictive requirement. In this work the possibility of redesigning the structure before controlling it is explored. Intuitively this appears to be a better approach to the overall problem. Simultaneous structural optimization and control as has been proposed by some investigators (Refs. [1-7]) may even be better. In these simultaneous structural design and control problems, a composite functional stemming from a weighted combination of structural weight and the usual quadratic performance index from optimal control theory are minimized. However, the questions about selection of appropriate weighting matrices in arriving at the composite functional are still unresolved.

Because of these aforementioned difficulties, in the present approach, a performance index is selected, and a control law that minimizes this performance index is determined for a given set of initial conditions, using the optimal control theory. The structure is then optimized and the minimum of the same performance index with identical initial conditions is determined, again using the optimal control theory. The minima obtained in the two cases are compared to see if any improvement is achieved. Specifically, the ratio of the minimum performance index of the unoptimized structure to that of the optimized structure is taken to be the measure of improvement achieved as a result of optimization.

Two optimization objectives are considered. In the first case, the fundamental frequency of the structure is maximized subject to frequency

separation constraints. In the second case the sum of the squares of the difference between the structural frequencies and of certain predefined target frequencies is minimized. In both cases, an upper limit on the structural mass is imposed. Maximization of fundamental frequency of a structure subject to constraint on maximum mass leads to configurations that exhibit frequency coalescence. Imposing frequency separation constraints avoids this problem, as the frequencies are kept apart during the optimization process.

The quadratic performance index of the control theory is a function of the initial conditions and certain scaling parameters, that are specified by the designer. The effects of different scaling parameters and initial conditions on the improvement in the performance index obtained by optimization are considered.

For the purposes of illustration a stiffened laminated composite panel is selected. The number of plies with a given orientation is one set of design parameters while the stiffener areas form the second set of design parameters. The number of plies can take on only integral values while the stiffener areas can take any continuous values. The combined set of design parameters has therefore integer and continuous design parameters. The structural optimization problem considered therefore belongs to the class of non linear mixed integer programming (NMIP). In structural design, when design parameters that can assume only integral or discrete values are encountered, the easiest procedure is to solve the problem treating these variables as continuous and then rounding them off to the nearest integer. This procedure though simple

to implement can lead to designs that are not only suboptimal but also infeasible. On the other hand Integer Programming algorithms are rather time consuming and need several continuous optimization problems to be solved. Measures to accelerate the continuous sub-problem optimizations are therefore essential.

Chapter 2 presents a brief literature survey of relevant topics. Chapter 3 discusses the structural optimization, and control methods used in this study. Details needed to calculate derivatives of frequencies with respect to the design variables are also discussed.

Numerical results are given in Chapter 4.

Appendix A discusses the Dakin's algorithm used to solve the integer programming problem. This algorithm needs the solution of a number of continuous programming problems. These continuous programming problems are solved using the Variable Metric Method for Constrained Optimization (VMCON). This algorithm is discussed in Appendix B.

To compute the performance index for an optimized and an unoptimized structure IMSC (Independent Modal Space Control) is used, because of its computational advantages and robustness. Computational details of this technique are given in Appendix C.

To compute the vibration frequencies of the structure, FEM discretization is employed. The laminated plate is modelled using isoparametric plate bending elements, while the stiffeners are modelled using frame elements. Appendix D provides the relevant element mass and stiffness matrices.

The methods used to compute eigenvalues and eigenvectors are presented in Appendix E.

It is hoped that the Appendices will save the reader the trouble of wading through unnecessary details, and also provide quick reference material when needed.

CHAPTER 2

LITERATURE SURVEY

2.1 Simultaneous Structural Optimization and Control

The conventional approach to structural design and control is essentially uncoupled. That is, a nominal structural design is established, and then the control system design is undertaken for a specified structural model. In recent years, this situation is steadily changing. A brief review of this emerging trend follows.

Hale and Lisowski [1,2] have considered the problem for simple structures. The feedback gains are calculated using optimal control which necessitate the solution of the Riccati equation. The main difficulty encountered in the formulation of Hale's algorithm is the relatively high order of the resulting non-linear two-point boundary value problem, which must be solved at each state of the iterative redesign procedure.

Messac and Turner [3] consider the problem of simultaneously optimizing the structural and control design. Finite element method is used to discretize the continuous system into a finite system of order n. Modal summation is used to represent the system and only p modes out of the original n modes are retained, where p is much less than n. The control forces applied are assumed to be a function of all the p modes, and the corresponding linear quadratic optimal control problem requires the solution of a coupled, non-linear matrix Ricatti equation of order 2p in the steady state case. A numerical example is considered for the

case of an axial rod, discretized using 20 extensional finite elements, resulting in 21 degrees of freedom.

Khot, Venkayya and Eastep [4], [5] show that by designing a structure based on an optimality criterion approach the dynamic characteristics of a closed-loop system of a large space structure (LSS) can be improved. The optimality criterion used in this study seeks to minimize static displacements associated with the line of sight (LOS) error. The optimal control problem is then formulated in the physical space (as opposed to the modal space). The associated coupled non-linear matrix Ricatti equation is of order 2n, in the steady state case, n being the order of the finite element model used to discretize the original continuous system. A truss structure having twelve degrees of freedom is considered. The dynamic properties of the optimized and the unoptimized structure are compared, showing that the optimized structure has an improved performance.

Junkins, Bodden and Turner [6], [7] derive expressions for eigenvalues of the closed loop system with respect to the design variables which include structural parameters, sensor/actuator locations and control gains. Two variations of a basic approach are considered. Firstly, the case of direct linear output feedback control law is addressed. Secondly, the case of a steady state quadratic regulator control law is considered. For both cases an eigenvalue placement/optimization approach is used to solve approximately a sequence of minimum design modification problems. Numerical results are

presented for the Draper RPL Configuration [6], discretized using the assumed modes method.

In [9], Salama, Hamidi, and Demsetz have considered a different approach to the vibration regulation problem. They seek to minimize the sum of a mass penalty term and a quadratic cost functional subject to both state variable inequality constraints and structural parameter constraints.

Hale [10] considers an ellipsoidal set-theoretic approach to the inegrated structural/control synthesis for vibration regulation of flexible structures. The synthesis attempts to maximize the allowable magnitude of an unknown but bounded disturbance to the structure while explicitly satisfying specific input and output constraints. Both structural parameters and control gains are variable during a search for the maximum allowable disturbance.

Haftka, Martinovic and Hallauer [11,12] describe a procedure for checking whether small changes in a structure have a potential for significant enhnacements of its optimized vibration control system. The control system is optimized for maximum performance for the original structural configuration, and then reoptimized to take full advantage of the structural modifications. Analytic predictions are validated experimentally.

Lamberson and Young [13] use a lattice plate finite element based on a continuum model for a large plate-like lattice space structure to examine the effect of variation of several structural parameters on the

natural frequencies, mode shapes and the resulting control system performance, while the total mass of the structure is held constant.

2.2 Structural Optimization

2.2.1 Optimization with Integer Variables

Cutting plane methods are probably the first systematic techniques available for the solution of the integer (linear) problems. The early works of Dantzig, Fulkerson and Johnson [14] directed the attention of researchers to the importance of solving linear integer programming problems. Markovitz and Manne [15] considered the more general case of discrete variables. Dantzig [16] was the first to propose the cutting plane method for linear integer problems. However, there is no guarantee that his method would converge to the integer solution in a finite number of steps. The first cutting plane method, that guaranteed an integer solution in a finite number of steps was by Gomory [17]. Although this algorithm converged in a finite number of steps, it ran into difficulties caused by machine roundoff. A new algorithm was developed by Gomory [18] to overcome, precisely, the above problem. Gomory [19] extended the above methods to cover mixed integer problems. Glover [20] introduced a new type of cutting plane method known as the bound escalation method. Subsequently, Young [21], Balas [22] and Glover [23] developed what is known as the "convexity" cut method.

The above cutting plane methods are all of the dual type; that is, instead of solving the original problem (the primal problem) a new (dual) problem is generated using suitable transformations. Solving

this new (dual) problem provides a solution to the original (primal) problem. This method is resorted to, when the dual problem lends itself to a more efficient solution as compared to the original problem. Drawback of this method lies in the fact that the solution to the problem is not available until the algorithm converges. This is a major disadvantage if calculations are stopped prematurely. A primal algorithm was first introduced by Ben-Israel and Charnes [24], however, the first finite (a problem that converges in a finite number of steps) primal algorithm was developed by Young [25]. Improvements on these algorithms were given by Young [26] and Glover [27].

The cutting plane methods, both primal and dual are only applicable to linear (pure or mixed) integer problems as they are inherently based on linearity assumptions. In contrast, the branch and bound algorithms are not based on any such linearity assumptions. However, when required, linearity of the problem can be easily exploited in the branch and bound formulations.

The underlying theory for the branch and bound algorithm was first presented by Bertier and Roy [28]. Balas [29] repeated their theory in a simpler form. Later Mitten [30] generalized and extended Bala's work. The first known branch and bound algorithm was developed by Land and Doig [31] as an application to the mixed and pure integer problem. The branch and bound algorithm as proposed by Land and Doig is highly impractical for computer implementation as it requires a large amount of computer memory. Secondly, the problem assumes linearity, in its formulation. Dakin [32] modified the Land and Doig algorithm to

facilitate computer implementation, and also to make it applicable to non-linear mixed integer programming problems.

Gupta [33], Gupta and Ravindran [34] use numerical results to show that Dakin's algorithm is well suited to solve relatively large, nonlinear mixed integer programming problems. As stated in Chapter 1 the present study uses this algorithm for the solution of the nonlinear, mixed integer structural optimization problem.

2.2.2 Structural Optimization with Integer Variables

Many variables entering into engineering design problems, are restricted to assume only discrete values. Examples of such variables are numbers of items, such as the number of stiffeners on a plate, the number of transverse bulkheads on a ship, the number of bars in a truss etc. In recent years a number of researchers in the field of strucutral optimization have turned their attention to the problem wherein some or all of the design variables may assume only integral or discrete values [35-40].

Schmit and Fleury [35] use approximation concepts and dual methods to solve structural synthesis problems involving a mix of discrete and continuous type sizing type of design variables. The basic mathematical programming statement of the structural synthesis problem is converted into a sequence of explicit approximate primal problems of separable form. These problems are solved by constructing continuous explicit dual functions, which are maximized subject to simple nonnegativity constraints. There is no guarantee however that the dual methods will yield the optimum solution to the discrete problem due to the fact that

it is not convex. However, results presented in [35] are encouraging. Imai [36] uses the above concepts to the problem of material selection.

Hua [37] uses an implicit enumeration scheme for finding the minimum weight design of a structure with discrete member sizes. A simplifying assumption is made, namely that, if reducing the size of a member causes an originally feasible solution to become infeasible, further reducing the size will not make the structure feasible. No basis for this assumption is stated. Johnson [38] uses a branch and bound algorithm to find the minimum weight design of a rigid-plastic structure with discrete sizes. Linking of elements is done to reduce the number of design variables. The objective function and the constraints are lienar functions of the design variables, making it possible to use linear programming techniques to obtain the solution to the continuous problem. Linearity assumptions are used to formulate branching and bounding rules to force the design variables to discrete values.

Gisvold and Moe [39] use a penalty method approach to minimize the weight of a structure with two discrete variables. The objective function that is to be minimized is augmented by a term that is positive everywhere and vanishes at the discrete points.

Templeman and Yates [40] use a segmental method for the discrete design of a minimum weight structure. The problem of finding the discrete sizes of the cross-sectional areas is converted to one of finding the continuous lengths of element segments each having one of the possible discrete cross-sectional areas. The resulting continuous

optimization problem is solved using linear programming, and its weight is taken to be the lower bound on the structural weight obtainable with discrete sizes. Use is made of the linearity of the problem considered to force discrete design variables to assume discrete values.

2.2.3 Structural Optimization with Continuous Variables

Mathematical programming was first applied to structural optimization problems by Prager [41] and Livesley [42]. Schmit's work [43] on structural synthesis and his subsequent efforts laid a firm foundation to modern numerical structural optimization. Moses [44] developed the technique of sequential linear programming (SLP). Structural optimization developed along two differing lines, namely, mathematical programming and optimality criteria methods. From the beginning mathematical programming algorithms (MPA) relied on rigourous mathematical procedures but consumed a lot of computer resources while optimality criteria methods (OCM) were intuitive in nature but had the advantage of converging very fast. Venkayya and his collaborators [45] started the development of optimality criteria approaches along with Prager [46], and Taylor [47]. Kicher [48] compares the two methods, while the work of Fleury and Sander [49] and Fleury and Schmit [50] shows the relationships between the two methods.

Several techniques were developed to reduce the computational time. Some were of a general nature while others were to be used for specific applications. Schmit [51] proposed approximation concepts while Haftka and Yates [52,53] developed fast reanalysis algorithms for flutter calculations.

Over the years a number of Mathematical Programming algorithms have been successfully used in structural optimization. The following is a brief overview of some of these algorithms.

Rosen's gradient projection method is based on projecting the search into the subspace tangent to the active constraints [54]. The basic assumption of the gradient projection technique is that the search is carried out in the subspace defined by the active constraints. The solution therefore proceeds along the constraint boundaries. The gradient projection method has been generalized by Rosen [55] to nonlinear constraints. The method is based on the linearization of the constraints at the solution point. The main difficulty caused by the nonlinearity of the constraints is that the solution typically moves away from the constraint boundaries. Some restoration moves are therefore necessary to move back to the curved constraint boundaries.

The feasible directions method [56] has the opposite philosophy to that of the gradient projection method. Instead of following the constraint boundaries, the solution procedure tries to stay away from them while at the same time trying to minimize the objective function. The method of feasible directions has been programmed in packages such as CONMIN [57] and ADS-1 [58] which are widely used for structural optimization.

Penalty methods replace the constrained optimization problem by an unconstrained one. The exterior penalty method applies penalties for violation of the constraints [59]. The main disadvantage with these methods is that the penalty is defined only in the infeasible domain.

The intermediate designs are infeasible, and if the solution is stopped prematurely the design may be useless as it is infeasible.

The interior penalty methods on the other hand keep the design in the feasible domain, however, they require an initial design that is feasible. The common form of the interior penalty function is the reciprocal of the constraint value. It can be easily seen that as the constraint boundary is reached the penalty term becomes infinitely large. If the initial design is in the feasible domain than the penalty term will keep it away from the constraint boundary. However, if the design point is in the infeasible domain, the contribution from the inverse penalty term will be negative, which is quite meaningless. The inverse penalty function, used in the interior penalty formulation is therefore applicable only as long as the design remains in the feasible region. In several structural optimization problems, obtaining a feasible design may be a difficult task. For these reasons there has been an increasing use of extended interior penalty functions. These penalty functions combine the inverse interior penalty function in most of the feasible domain with an exterior continuation. The contribution from the penalty terms for constraint violation is thus kept positive. The exterior continuation can be linear [60], however, the resulting function that needs to be minimized has first derivative discontinuity.

Haftka and Starnes [61] avoid this difficulty by using a quadratic continuation, in which up to second derivative continuity exists. Second derivative continuity makes it possible to use the Newton's method for the resulting unconstrained minimization. In their work the

second derivatives needed for the Newton's method have been calculated approximately, using first derivative information and the fact that at the constraint boundaries the resulting augmented function has large curvatures. A cubic and variable order extended penalty function has also been proposed [62]. Another combination of interior and exterior penalty functions occurs when an exterior function is used for equality constraints and an interior one for inequality constraints [63]. The Fortran code NEWSUMT [64] developed by Miura and Schmit is based on an extended interior penalty function and Newton's method with approximate second derivatives.

Multiplier methods combine the use of Lagrange multipliers with that of penalty functions. When only Lagrange multipliers are employed the optimum is a stationary point rather than a minimum of the Lagrangian function. When only penalty functions are employed a minimum is obtained but ill-conditioning is also present. By combining the two techniques an unconstrained problem is obtained where the function to be minimized does not suffer from ill-conditioning [65].

The addition of penalty terms of the Lagrangian function by multiplier method convert the optimum from a stationary value of the Lagrangian function to a minimum of the augmented Lagrangian. Projected Lagrangian methods [66] achieve the same result employing a different technique. They are based on a theorem which states that the optimum is a minimum of the Lagrangian function in the subspace of vectors orthogonal to the active constraint gradients. Projected Lagrangian methods employ a quadratic approximation to the Lagrangian in this

subspace. The direction seeking algorithm requires the solution of a quadratic programming problem (quadratic objective function, linear constraints). The VMCON algorithm (see Appendix B) used in this work is based on the projected Lagrangian method.

For linear problems the solution to the original constrained optimization problem may be obtained by solving the so called dual problem, in which the Lagrange multipliers are the unknowns. The primal space methods treat the original design variables as unknowns so that efficiency is easily influenced by the number of design variables. The dual space methods, on the other hand, seek for the optimum Lagrange multipliers for selected potentially critical constraints so that the efficiency depends on the number of the potentially critical constraints. Since there are relatively few critical constraints at an optimum, the problem size in the dual space generally tends to be smaller than the primal space dimension. There are several ways of generalizing the linear dual formulation to nonlinear problems. In applications to structural optimizations, the most successful has been one due to Falk [65] as specialized to separable problems by Fleury [67]. The dual formulation produces an optimum to the original problem only when the problem in convex. Secondly, the dual problem is computationally cheaper to solve only in the case of separable problems [59]. The dual method can be used in conjunction with certain approximation conepts and has been used successfully in developing the ACCESS-3 computer program by Schmit and co-workers [68].

Closely related to the dual methods are the optimality criteria methods [45]. The optimality criteria methods consist of two complimentary components. The first is the stipulation of the optimality criterion. One can choose rigorous mathematical criteria, such as the Kuhn-Tucker conditions or an intuitive one such as the stipulation that the strain energy density in the structure be uniform [49]. The second component is the algorithm which is used to resize the structure in the expectation that it will lead to the satisfaction of the optimality criteria. Again, one may use a rigorous mathematical method to achieve the satisfaction of the optimality criteria or one may devise an ad hoc procedure which may or may not work. Some of the intuitive optimality criteria methods used include the Fully Stressed Design [68,69] and the uniform stran energy [45]. The optimality criteria methods have been used quite successfully in the design of composite structures with stress and displacement constraints [70] as well as for structures with specified eigenvalue distribution [71].

Several researchers developed techniques suited to specific problems. Nshanian et al. [72] consider the problem of minimizing the stresses in a laminated plate while Hirano [73] and Nshanian et al. [74] consider the problem of maximizing the buckling load (or the fundamental frequency). Khot et al. [70] study the minimum weight design of a laminated plate subject to stress and displacement constraints. In all these studies, the ply thickness is taken to be a variable, that may assume any continuous value.

2.3 Structural Control

In aerospace applications control theories [75-80] were successfully used, at first, to control the motion and the resulting trajectory of space vehicles. An example is the control of Saturn V booster-vehicle motions during the launch phase, where the booster-vehicle is subjected to random wind-loads [81,82]. Later, Bender, Karnopp, Sevin etc. [83,84,85] applied different control methods to suppress structural vibrations.

Theoretical studies of structural control follow two different approaches. The independent modal space control (IMSC) method [86] and the coupled control method [77]. Meirovitch [87] compares various control techniques for large flexible systems. Structural control literature reflects the many practical design difficulties encountered in implementation. For example Van Landingham et al. [88] and Meirovitch et al. [89] consider the problem of the number of actuators to be used and their placement.

The modal control methods mentioned above can be used for linear structures for which an eigenvalue problem can be solved to obtain the structural frequencies. Kamat [90] uses an extension of the method suggested by Narendra and Tripathy [91] to study the optimal control of a beam in nonlinear response. This method involves the direct minimization of the performance index using mathematical programming techniques.

The number of experimental studies in structural control is surprisingly small. References [92]-[97] represent some of the

significant experimental work in control. All of these rferences, however, report significant practical difficulties encountered in attempts to implement control strategies. Hallauer et al. [98] report some of the first successful attempts using direct velocity feedback control (DVFC), where experimental results are compared with theoreitcal predictions. Meirovitch et al. [99] report the results of using nonlinear natural control in conjunction with IMSC to suppress beam vibrations.

CHAPTER 3

STRUCTURAL OPTIMIZATION AND CONTROL-THEORETICAL BASIS

3.1 Structural Optimization

A structural optimization problem can be stated as follows

$$\text{Minimize } f(x),\ x = (x_1, x_2, \ldots, x_n) \tag{3.1.1}$$

$$\begin{aligned} \text{Subject to } h_i(x) &= 0 \quad i = 1,2,\ldots,n_e \\ g_i(x) &\geq 0 \quad j = 1,2,\ldots,n_g \end{aligned} \tag{3.1.2}$$

The vector x will be referred to as the design variable vector. For structural optimization problem, it normally represents some characteristics of structural elements such as cross-sectional diameters, area etc. If f, h_i and g_j are all linear functions of the design variable x the problem is a linear programming problem (LP). If any of the f, h_i or g_j are non-linear functions of x, a nonlinear programming problem (NLP) results. If all the design variables are such that they can assume any real values within specified bounds then one has the classical continuous variable optimization problem. In several structural design problems, however, some or all of the design variables may assume only integer or discrete values. Such problems can be formulated as non-linear mixed integer programming problems (MIP). For example the number of blades on a compressor or a turbine, number of plies in a composite laminate or the number of control actuators to be used on a structure are all examples of design parameters that can take only integer values. Market availability and standardization also forces engineers to look at parameters that may assume certain

"discrete" values. These values though discrete are not necessarily integers. The mixed discrete optimization problem is therefore a more general problem than the mixed integer programming (MIP) problem. However it is possible to convert a discrete optimization problem into an MIP problem quite easily, as follows.

Suppose a variable z_j is allowed to take on only one of several values, say v_1, v_2, v_N. This is equivalent to setting

$$z_j = x_1 v_1 + x_2 v_2 + \ldots + x_N v_N \tag{3.1.3}$$

with

$$x_1 + x_2 + \ldots + x_N = 1 \tag{3.1.4}$$

and

$$x_j = 0 \text{ or } 1 \quad (j = 1, \ldots, N) \tag{3.1.5}$$

It is feasible to solve an MIP problem in an approximate way by relaxing the integrality constraints on the integer variables and then rounding them off to the nearest integer value. This procedure although simple to implement has a shortcoming. This is due to the fact that the solution obtained by rounding off may be not only sub-optimal but also infeasible. Also the task of obtaining an integer feasible solution may be a nontrivial one.

Integer programming techniques are generally categorized into two broad types: (1) search methods and (2) cutting plane methods. The first type is motivated by the fact that the integer solution space can be regarded as consisting of a finite number of points. In its simplest form, search methods seek the enumeration of "all" such points. This would be equivalent to a simple exhaustive enumeration. However, what

makes search methods more promising than simple exhaustive enumeration, is that the techniques have been developed to enumerate only a portion of all candidate solutions while automatically discarding the remaining points because they are either infeasible or inferior to points which are retained. The efficiency ofthe resulting search algorithms depends on the power of such techniques that discard the nonpromising solution points.

Search methods primarily include implicit enumeration techniques and branch-and-bound techniques. The first type is mostly suited for the "zero-one" problem, wherein the integer design variables may take on values of either zero or one. Even though, every discrete or integer problem can be converted into a zero-one problem as shown in Eqs. (3.1.3) through (3.1.5) it is clear that such a conversion increases the dimensionality of the problem, several fold, in most cases where the problem is not originally a zero-one problem. Hence, implicit ennumeration techniques are not suited for discrete or integer problems which are not of the zero-one type as posed.

Cutting methods are developed primarily for the solution of (mixed or pure) integer linear programming problem. These methods are motivated by the fact that the simplex solution to a linear program must occur at an extreme point. The idea then is to add specially developed secondary constraints that are violated by the current noninteger solution but never by any feasible (integer) point. The successive application of such a procedure should eventually result in a new solution space with its optimum extreme point properly satisfying the

integrality condition. The name "cutting" methods is suggested by the fact that the secondary constraints "cut" off infeasible parts of the continuous solution space.

The cutting plane methods, at present are adapted specifically to linear integer problems and cannot be used for nonlinear integer problems.

The branch and bound methods can be used to solve linear or nonlinear integer problems. The branch and bound procedure does not deal directly with the integer problem. Rather, it considers a continuous problem obtained by relaxing the integer restrictions on the variables. Thus the solution space of the integer problem is only a subset of the continuous space. The prime reason for dealing with the continuous problem is that it is simpler to manipulate such a problem. Furthermore, one can draw upon the tremendous advances in the theory of continuous optimization methods.

If the optimal continuous solution is integral, then it is also optimum for the integer problem. Otherwise, the branch and bound technique is applied by implementing two basic operations.

(a) Branching: This partitions the continuous solution space into subspaces (subproblems), which are also continuous. The purpose of partitioning is to eliminate parts of the continuous space that are not feasible for the integer problem. This is achieved by imposing (mutually exclusive) constraints that are necessary conditions for producing integer solutions, but in a way that no feasible integer point is eliminated. In other words, the resulting collection ofsubproblems

completely defines every feasible integer point of the original problem. Because of the nature of the partitioning operation, it is called branching.

(b) Bounding: Assuming the original problem is of the minimization type, the optimal objective value for each subproblem objective value for each subproblem created by branching sets a lower bound on the objective value associated with any of its integer feasible values. This bound is essential for "ranking" the optimum solution of the subsets, and hence in locating the optimum integer solution.

Dakin's algorithm used in this work is essentially an extension of the branch and bound algorithm proposed by Land and Doig [31,32] for the solution oflinear-programming problems in which some of the design variables are required to be integers. The Land and Doig algorithm is unsuitable for general nonlinear mixed integer programming problems on two counts. Firstly, it employs a tree structure that requires excessive computer storage [100], and secondly the branching rules are tied to the assumption of linearty [101].

Dakin's modification (see Ref. [32]) of the Land-Doig algorithm makes the branching rule independent of the linearity condition. The algorithm starts by finding a solution to the continuous problem wherein the integrality requirments are relaxed. If this solution is integral, then it is the optimal solution to the given discrete problem. If the solution is nonintegral then at least one integer variable, say x_k, is nonintegral, and takes the value, say b_k which can be divided into integral and fractional parts [b] and f respectively as

$$b_k = [b] + f \tag{3.1.6}$$

where [b] is integral and $0 < f < 1$. If x_k has to take an integer value then either one of the following two conditions must be satisfed.

$$x_k \leq [b] \tag{3.1.7}$$

or

$$x_k \geq [b] + 1 \tag{3.1.8}$$

Constraint conditions expressed by Eqs. 3.1.7, 3.1.8 clearly have nothing to do with linearity, and as such can be used to solve nonlinear mixed integer programming problems. Details of the Dakin's algorithm can be found in Appendix A.

3.2 Application to a Vibrating Stiffened Composite Plate

In the active control of large space structures built-up from fiber reinforced composite materials it will be necessary to avoid undesirable control coupling effects due to closely spaced frequencies. This will require the placement of a lower limit on one or more of the natural frequencies of vibration or a specification of an appropriate separation of the lower frequencies. It is with this objective in mind that the problem is addressed.

Two optimization objectives are considered. In the first case, the fundamental frequency of the structure is maximized with separation constraints on other frequencies. In the second case the sum of the squares of the differences between the structural frequencies and of certain predefined target frequencies is minimized. In both cases the design is subject to

1. Upper bound on structural weight

and

2. A specific frequency separation

(i.e., the ratio ofthe second, third, fourth frequencies to the first frequency is required to exceed a certain prescribed ratio, r, r > 1). The laminate is assumed to be of a symmetric construction. The number of plies of a specified orientation and the areas of the stiffeners are the integer and continuous design variables respectively. Each ply is assumed to be of uniform thickness t_1. Below the mid plane the construction is such so as to give a symmetric lay out. As an example, the following laminate construction (starting from the first layer up to the mid plane) is assumed.

n_1 plies at 90°

n_2 plies at 75°

n_3 plies at 60°

n_4 plies at 45°

n_5 plies at 30°

n_6 plies at 15°

n_7 plies at 0°.

n_1, n_2, n_3,...,n_7 form the 7 integer variables of the problem. Finite element discretization is then used to determine the structural mass and stiffness matrices and an eigenvalue problem is solved to get the eigenvalues and the eigenvectors.

The simply supported laminated plate of Fig. 1 is divided into 16, 8-noded, shear deformable, isoparametric, penalty plate bending elements [102]. Figure 1 shows the complete stiffened composite plate, with

stiffeners placed symmetrically about the laminate mid-plane. Each of the six stiffeners is divided into 8 frame elements. The 48 frame elements are divided into 8 groups through linking. Within each group all the elements have the same area A_i. Figure 2 shows the elements corresponding to a given continuous design variable (area) A_i. This grouping (linking) of elements was chosen on the basis of symmetry considerations.

Without linking of the element areas, there would have been 48 continuous design variables, corresponding to each frame element area, thereby greatly increasing the size of the optimization problem. This would have resulted in a prohibitive increase in computational time.

For each frame element the area A_k is assumed to be related to its moment of inertia I_k by the relation

$$I_k = \alpha(A_k)^n$$

where

$$\alpha = \left(\frac{I_o}{A_o^n}\right)$$

and n = 3 for the problem.

Because of the global nature of the frequency constraints involved and the absence of local constraints such as stress constraints it suffices to use cross-sectional area and moment of inertia design variables.

3.2.1 One Optimization Scheme

With these preliminaries the optimization problem for the plate of Figure 1 can be stated mathematically in a non-dimensional form as

$$\text{Maximize } \left(\frac{\lambda_1}{\lambda_o}\right)^2 \tag{3.2.1.1}$$

$$\text{Subject to } \left(\frac{\lambda_{i+1}}{\lambda_{o1}}\right)^2 \geq r_i \quad , \quad i = 1,2,\ldots,7 \tag{3.2.1.2}$$

$$\Sigma n_i = 12 \tag{3.2.1.3}$$

$$\Sigma a_i m_i \leq 2 \tag{3.2.1.4}$$

$$0 \leq n_i \leq 6 \tag{3.2.1.5}$$

$$0.0 < a_i \leq 1.0 \tag{3.2.1.6}$$

$$\begin{gathered} n_1, n_2, \ldots, n_7 \text{ are integers} \\ m_i = 1 \text{ for } i = 1,2,4,5 \\ m_1 = 0.5 \text{ for } i = 3,4,7,8 \end{gathered} \tag{3.2.1.7}$$

where λ_i is the ith frequency (expressed in rad/sec) of the structure shown in Fig. 1 and f_o is the frequency of the initial design. $r_i > 1$ are prescribed ratios, n_i is the number of plies having orientation θ_i, A_i
is the dimensional area and

$$a_i = \left(\frac{A_i}{A_o}\right)$$

is the nondimensionalized area of the ith stiffener (see Fig. 2) with A_o being a given reference area.

3.2.2 A Second Optimization Scheme

The optimization problem described by Eq. (3.2.1.1) through (3.2.1.7) is but one way of optimizing the structure. To study the impact of different optimization schemes on structural control performance a second optimization scheme was implemented. It can be

stated mathematically as follows

$$\text{Minimize} \sum_{i=1}^{7} \left(\frac{\lambda_i}{\beta_i} - 1\right)^2 \qquad (3.2.2.1)$$

$$\text{Subject to } \left(\frac{\lambda_i + 1}{\lambda_0}\right) \geq r_i \quad i = 1,2,\ldots,7 \qquad (3.2.2.2)$$

$$\Sigma n_i = 12 \qquad (3.2.2.3)$$

$$\Sigma a_i m_i \leq 2 \qquad (3.2.2.4)$$

$$0 \leq n_i \leq 6 \qquad (3.2.2.5)$$

$$0.0 < a_i < 1.0 \qquad (3.2.2.6)$$

$$n_1, n_2, n_3, \ldots, n_7 \text{ are integers}$$

$$m_i = 1 \text{ for } i = 1,2,4,5$$
$$m_i = 0.5 \text{ for } i = 3,4,7,8 \qquad (3.2.2.7)$$

where $\beta_i > \lambda_i$ are prescribed numbers.

3.2.3 Derivatives of Vibration Frequencies with Respect to Design Variables

Efficient optimization codes such as VMCON (see Appendix B) using mathematical programming require the derivatives of the objective function and the constraints. For the problem considered, the objective function and the constraints are in terms of frequencies. In this section, details of calculating the derivatives of frequencies with respect to the design variables are presented.

The simplest and most straightforward way to compute the derivatives is by using finite differences. Specifically, if one uses the forward difference scheme,

$$\frac{\partial \lambda_i}{\partial x_j} = \frac{\lambda_i(x_j + h) - \lambda_i(x_j)}{h} \qquad (3.2.3.1)$$

The main disadvantage of the finite difference scheme is that it requires the solution of an eigenvalue problem once for each design variable. This is a computationally expensive process. Secondly, to get a reasonable value for the computed derivative, the eigenvalue problems need to be solved to a very high degree of accuracy.

Calculation of frequency derivatives using analytical formulae is computationally cheaper and does not require the solution of any additional eigenvalue problems other than to compute the frequencies and eigenvectors.

Derivative of the ith frequency λ_i with respect to the jth design variable x_j is given by the relation (see Ref. 59)

$$\frac{\partial \lambda_i}{\partial x_j} = U_i^T \left(\frac{\partial K}{\partial x_j} - \lambda_i \frac{\partial M}{\partial x_j}\right) U_i \qquad (3.2.3.2)$$

where U_i = ith eigenvector

K = stiffness matrix

M = mass matrix

In this work, the number of plies with a given orientation and the stiffener areas are the two sets of design variables. Calculation of $\frac{\partial K}{\partial x_j}$ with respect to each of these two sets of design variables is presented next.

The global matrices K, M are assembled from the element matrices. To differentiate K, M it is sufficient therefore to assemble the matrices obtained by differentiating the element stiffness matrices.

This, in turn requires the differentiation of matrices A, D defined by Eq. (D.1.6). For convenience, consider a six ply laminate as shown in Fig. 4. We have

$$\begin{aligned} z_1 &= -(n_1 + n_2 + n_3)t \\ z_2 &= -(n_2 + n_3)t \\ z_3 &= -n_3 t \\ z_4 &= 0 \end{aligned} \tag{3.2.3.3}$$

where t denotes individual ply thickness.

For a symmetric laminate

$$A = 2\{\bar{Q}^1(z_2 - z_1) + \bar{Q}^2(z_3 - z_2) + \bar{Q}^3(z_4 - z_3)\} \tag{3.2.3.4}$$

$$D = \frac{2}{3}\{\bar{Q}^1(z_2^3 - z_1^3) + \bar{Q}^2(z_3^3 - z_1^3) + \bar{Q}^3(z_4^3 - z_3^3)\} \tag{3.2.3.5}$$

$$\frac{\partial A}{\partial n_j} = 2\{\bar{Q}(\frac{\partial z_2}{\partial n_j} - \frac{\partial z_1}{\partial n_j}) + \bar{Q}^2(\frac{\partial z_3}{\partial n_j} - \frac{\partial z_2}{\partial n_j}) + \bar{Q}^3(\frac{\partial z_4}{\partial n_j} - \frac{\partial z_3}{\partial n_j})\} \tag{3.2.3.6}$$

$$\begin{aligned} \frac{\partial D}{\partial n_j} = 2\{&\bar{Q}^1(z_2^2 \frac{\partial z_2}{\partial n_j} - z_1^2 \frac{\partial z_1}{\partial n_j}) + \bar{Q}^2(z_3^2 \frac{\partial z_3}{\partial n_j} - z_2^2 \frac{\partial z_2}{\partial n_j}) \\ &+ \bar{Q}^3(z_4^2 \frac{\partial z_4}{\partial n_j} - z_3^2 \frac{\partial z_3}{\partial n_j})\} \end{aligned} \tag{3.2.3.7}$$

and

$$\frac{\partial z_i}{\partial n_j} = \begin{bmatrix} \frac{\partial z_1}{\partial n_1} & \frac{\partial z_1}{\partial n_2} & \frac{\partial z_1}{\partial n_3} & \frac{\partial z_1}{\partial n_4} \\ \frac{\partial z_2}{\partial n_1} & \frac{\partial z_2}{\partial n_2} & \frac{\partial z_2}{\partial n_3} & \frac{\partial z_2}{\partial n_4} \\ \frac{\partial z_3}{\partial n_1} & \frac{\partial z_3}{\partial n_2} & \frac{\partial z_3}{\partial n_3} & \frac{\partial z_3}{\partial n_4} \\ \frac{\partial z_4}{\partial n_1} & \frac{\partial z_4}{\partial n_2} & \frac{\partial z_4}{\partial n_3} & \frac{\partial z_4}{\partial n_4} \end{bmatrix} \tag{3.2.3.8}$$

$$= t \begin{bmatrix} -1 & -1 & -1 & -1 \\ 0 & -1 & -1 & -1 \\ 0 & 0 & -1 & -1 \\ 0 & 0 & 0 & -1 \end{bmatrix} \tag{3.2.3.9}$$

To calculate $\frac{\partial M}{\partial K}$, it is sufficient to replace p, I by $\frac{\partial p}{\partial x}$, $\frac{\partial I}{\partial x}$. (See Eq. (D.1.3) for definition of p, I). For the six-ply, symmetric laminate, mentioned above

$$p = 2\{(z_2 - z_1)\rho^{(1)} + (z_3 - z_2)\rho^{(2)} + (z_4 - z_3)\rho^{(3)}\} \tag{3.2.3.10}$$

$$\frac{\partial p}{\partial n_j} = 2\{(\frac{\partial z_2}{\partial n_j} - \frac{\partial z_1}{\partial n_j})\rho^{(1)} + (\frac{\partial z_3}{\partial n_j} - \frac{\partial z_2}{\partial n_j})\rho^{(2)} + (\frac{\partial z_4}{\partial n_j} - \frac{\partial z_3}{\partial n_j})\rho^{(3)}\} \tag{3.2.3.11}$$

$$I = \frac{2}{3}\{(z_2^3 - z_1^3)\rho^{(1)} + (z_3^3 - z_2^3)\rho^{(2)} + (z_4^3 - z_3^3)\rho^{(3)}\} \tag{3.2.3.12}$$

$$\frac{\partial I}{\partial n_j} = 2\{(z_2^2 \frac{\partial z_2}{\partial n_j} - z_1^2 \frac{\partial z_1}{\partial n_j})\rho^{(1)} + (z_3^2 \frac{\partial z_3}{\partial n_j} - z_2^2 \frac{\partial z_2}{\partial n_j})\rho^{(2)} + z_4^2 \frac{\partial z_4}{\partial n_j} - z_3^2 \frac{\partial z_3}{\partial n_j})\rho^{(3)}\} \tag{3.2.3.13}$$

$\rho^{(1)}, \rho^{(2)}, \ldots, \rho^{(n)}$ are the layer densities. $\frac{\partial z_i}{\partial n_j}$ is given by relation (3.4.9).

3.3 Structural Control

One of the objectives of structural control is to suppress undesirable motion resulting from some unavoidable excitation such as onboard machinery or docking maneuvers. In active control the motion of the structure is sensed and suitable forces are applied to reduce and ultimately eliminate the undesirable motion. In optimal control, the forces are applied such that a preselected performance index is minimized. In order to be able to accomplish this a model capable of accurately determining the dynamics of the structure is essential. It is assumed here, that the continuous structure governed by a partial differential equation model is approximated by a finite set of ordinary differential equations, using finite element discretization.

For a discretized structure, the optimal control problem can be stated as follows

$$\text{Minimize } J = \frac{1}{2} v^T(t_f)Hv(t_f) + \int_{t_o}^{t_f} \frac{1}{2} [v^T(t)Q(t)v(t) + c(t)]dt \tag{3.3.1}$$

Subject to the state equations

$$\dot{v}(t) = A(t)v(t) + B(t)F(t) \tag{3.3.2}$$

H and Q are real symmetric positive semi-definite matrices, the initial time t_o and the final time t_f are specified, v(t) is the state vector

describing the position and velocity of the structure at time t, and F(t) is the control effort.

c(t) is the control cost that can be expressed as

$$c(t) = F^T(t)R(t)F(t) \tag{3.3.3}$$

where R is a positive definite matrix.

Solution of the control problem posed by Eq. (3.3.1) through (3.3.3) can be shown to be (see Ref. [77])

$$F(t) = -R^{-1}(t)B^T(t)G(t)x(t) \tag{3.3.4}$$

where G(t) satisfies the following Ricatti equation

$$\dot{G}(t) + Q(t) - G(t)B(t)R^{-1}(t)B^T(t)G(t) + G(t)A(t) + A^T(t)G(t) = 0 \tag{3.3.5}$$

with the final time condition

$$G(t_f) = H \tag{3.3.6}$$

For a structure discretized using the finite element method, the equations of motion with no damping can be written as

$$\underset{(nxn)(nx1)}{M\ddot{u}(t)} + \underset{(nxn)(nx1)}{Ku(t)} = \underset{(nx1)}{F(t)} \tag{3.3.7}$$

where u = deflection vector, M, K are the consistent mass and stiffness matrices respectively of order n. F is the vector of nodal forces.

Equation (3.3.7) can be written in the form of Eq. (3.3.2) by defining the state vector v to be of the form

$$v = \begin{Bmatrix} \dot{u} \\ u \end{Bmatrix} \tag{3.3.8}$$

and

$$A = \begin{bmatrix} A_{11} & A_{12} \\ A_{21} & A_{22} \end{bmatrix}$$

with

$$A_{11} = -M^{-1}K$$

$$A_{12} = A_{21} = [0] = \text{zero matrix of order n}$$

$$Z_{22} = In = \text{unit matrix of order n} \qquad (3.5.9)$$

If Q is chosen as

$$Q = \begin{bmatrix} Q_{11} & Q_{12} \\ Q_{21} & Q_{22} \end{bmatrix} \qquad (3.5.10)$$

with $Q_{11} = M$ = mass matrix

$Q_{22} = K$ = stiffness matrix

$Q_{12} = Q_{21} = 0$ = zero matrix of order n (3.5.11)

then the term $1/2\ v^T Q v$ in Eqs. 3.5.1 represents the sum of the strain energy and the kinetic energy of the structure.

For large order systems, such as considered in this work, the solution of the matrix Ricatti Eq. (3.5.5) is not feasible, due to difficulties encountered in numerical computations [87].

An alternate method, Independent Modal Space Control (IMSC) described in Ref. [86] is more suitable for large order systems. In this method, the control forces are specified in the modal space instead of the actual physical space. Also by suitably choosing the modal control forces, each mode of vibration is controlled independently of the other modes. The performance index in this case is chosen to be of

the form

$$J = \sum_{i=1}^{p} J_r \tag{3.3.12}$$

where p is the number of modes controlled and J_r is the performance index associated with the rth mode, and is defined as

$$J_r = \int_0^{t_f} (\omega_r^2 \xi_r^2 + \omega_r^2 \eta_r^2 + R_r z_{cr}^2)dt \tag{3.3.13}$$

where

$$\eta_r = \frac{\dot{\xi}_r}{\omega_r} \tag{3.3.14}$$

ω_r being the frequency (rad/sec) of the rth mode. The modal coordinates ξ_r (r = 1,2,...,p) are related to the displacement vector u, by the relation

$$u = X\xi \tag{3.3.15}$$

where X is the modal matrix, having as its columns the eigenvectors, obtained by the solution of the eigenvalue problem

$$KX = \omega^2 MX \tag{3.3.16}$$

ξ_r, η_r satisfy the constraint equations

$$\ddot{\xi}_r(t) + \omega_r^2 \xi_r(t) = z_{cr}(t) \tag{3.3.17}$$

$$\xi_r(t = 0) = \xi_r(0)$$

$$\dot{\xi}_r(t = 0) = \eta_r(0)\omega_r$$

Minimization of J_r in Eq. (3.5.12) with the differential constraint given by Eq. (3.3.17) leads to a 2x2 matrix Ricatti equation that can be

solved analytically (see Appendix C) for $t_f = \infty$. The parameter $R_r > 0$ in Eq. (3.3.13) is prescribed by the designer, and represents the penalty imposed on the control effort. A higher value of R_r will result in a smaller control force in the modal space, and vice versa.

An important aspect of IMSC is the fact that the modal control forces are independent of the actuator locations. The placement of actuators is thus a separate design step, and has been dealt with in the literature [89] quite extensively due to the fact that the magnitude of the actuator forces is strongly dependent on the actuator locations.

The method suggested in Ref. [103] is used to compute the actuator forces needed to control the lowest p modes, $p << n$. If F denotes the nodal force vector and F_p denotes the associated control vector, one can write

$$F = UF_p \tag{3.3.18}$$

in which U = a full rank n x p matrix with entries equal to either zero or one. The control vector F_p can be shown to be (see Ref. [103])

$$F_p = B^{-1}Z_c \tag{3.3.19}$$

where

$$B = x_p^T U \tag{3.3.20}$$

x_p being a nxp matrix having as its columns p lowest eigenvectors of the system described by Eq. (3.3.16). z_c = Modal Control Vector (see Appendix C, Eq. C.1.7).

CHAPTER 4

IMPLEMENTATION DETAILS AND NUMERICAL RESULTS

This chapter discusses measures undertaken to ensure an efficient implementation of the nonlinear mixed integer programming algorithm for the solution of the structural optimization problem. This is followed by a discussion of the impact of structural optimization on control of the stiffened laminated composite plate.

4.1 Implementation of Structural Optimization Algorithm

Dakin's algorithm is used to ensure that the integer design variables do take integral values. The continuous subproblems are solved using the code VMCON. Derivatives of frequencies needed for efficient solution of these subproblems are calculated using the analytic method described in Section 3.2.3. The continuous subproblems are defined by relations (3.2.1.1)-(3.2.1.7) or (3.2.2.1)-(3.2.2.7) with some additional constraints corresponding to eqs. (3.1.7), (3.1.8). These additional constraints are incorporated by modifying relation (3.2.2.5) or the corresponding relation (3.2.3.5) to

$$(\text{NMIN}) \leq n_i \leq (\text{NMAX}) \qquad (4.1.1)$$

The constraints resulting from the branching step, Eqs. (3.1.7) and (3.1.8) can be incorporated by suitably modifying the (NMIN) or (NMAX) vectors (the lower and upper bounds on the integer variables). During the process of successive branching if the lower and upper bounds, for the ith integer design variable coincide, then the corresponding variable is forced to take an integer value, say k i.e., $x_i = k$. For

the subproblem for which this happens, x_i is set to k and removed from the design space. For each variable taking on a specific integer value, the number of design variables is thus reduced by one, and the number of constraints described by Eq. (4.1.1.), by two. This reduces the subproblem size and hence the overall solution time considerably.

Table 1 provides the nodal coordinates and boundary conditions for the mesh used in the FEM discretization. Nodes are arranged in groups, and only the 1st, 2nd and the last node belonging to a group are listed. The coordinates of nodes not listed can be found by linear extrapolation of the coordinates of the first and second node in each group. The boundary conditions of the nodes not listed are identical to the boundary conditions of the 2nd node. For example in the 2nd group, only nodes 10, 11, and 14 are listed. Boundary conditions of nodes 12, 13 are identical to the boundary condition of node 11, while their coordinates can be found by linear extrapolation of coordinates of nodes 10 and 11. Table 2 provides the elastic constants of the material used for plate and frame element calculations. These properties are typical for plies made of graphite/epoxy [104]. Table 3 defines the initial design and its structural frequencies. The structural frequencies of the initial design are used to prescribe "reasonable" frequency separation constraints for the various optimization schemes. Table 4 provides a summary of the different optimization schemes considered. For the sake of convenience each of these schemes is given a specific name, to help in referring to them. OPT1a and OPT1b seek to maximize the fundamental frequency of the structure, subject to frequency

separation constraints defined in Table 5. Optimization schemes OPT2a through OPT2d seek to drive the structural frequencies to prescribed target frequencies. It was found that great care should be exercised in the selection of the target frequencies since any arbitrary choice was found to lead to numerical difficulties during optimization. The present choice of target frequencies was found to be reasonable. Schemes OPT2a through OPT2c differ only in that in each of these schemes the target frequencies are different. For all optimization schemes, except OPT1a, the bounds on the design variables and the frequency separation constraints are identical, and are defined in Table 6. Frequency separation constraints for OPT1a are defined in Table 5. Tables 7 and 8 provide the definition and solution of the structural optimization scheme OPT1a, OPT1b, respectively, as applied to the stiffened composite plate of Fig. 1.

4.2 Measures to Accelerate Sub-Problem Optimization

Depending on the number of integer design variables and their bounds it is necessary to solve a large number of structural optimization subproblems. A number of steps are taken to make the solution of the subproblems computationally efficient. Some of these steps involve using data computed during previous sub-optimizations. The steps involved may be listed as follows.

4.2.1 Removal of all Integer Variables, for which the Upper and Lower Bounds Coincide, from the Design Variable Space

The problem considered has 8 continuous design variables (the stiffener areas) and 7 integer variables, leading to a total of 15

design variables, for the subproblems. If 6 of the integer design variables take on fixed values and are removed from the design space then the subproblem has just 9 design variables. Also the number of constraints are reduced by 12 (2 for each design variable). A careful examination of Table 9 shows that considerable savings in computation time occurs when this procedure is adopted. The derivatives of the objective function and the constraints with respect to the design variables that have been removed need not be computed, and this involves savings in CPU time.

4.2.2 Storing of Certain Element Data to Avoid Repeated Integrations During the Assembly of Mass and Stiffness Matrices

As the geometry of the structural model does not change certain integration results computed during initial assembly of the structure can be stored for later use. This reduces the time to assemble the plate stiffness and mass matrices by a ratio of about six. It should be noted that the assembly of the stiffness and mass matrices needs to be performed once each time the frequencies are calculated. Also during the computation of derivatives one needs to perform the assembly for each design variable with respect to which the derivative is required.

4.2.3 Using Inverse Iteration Algorithms in Conjunction with Shifting and Derivative Data to Compute Required Frequencies Faster

It is possible to avoid computation of unneccessary intermediate frequencies. One can use inverse iteration to get the first frequency. If more than one frequency is needed the most commonly adopted practice is to use either of the following two schemes.

a) The first involves using subspace iteration in conjunction with Jacobi's method (see Appendix E). Suppose the 1st, 3rd and 8th frequencies are required. Then using the above method one would have to iterate with approximately 16 vectors, which would imply use of Jacobi iteration on a 16 by 16 matrix. This is rather time consuming. Also one is forced to work with all 16 eigenvectors even though only three are needed.

b) The second scheme involves using matrix deflation to get the higher frequencies. Matrix deflation however destroys the skyline structure of the mass and stiffness matrices. This would greatly increase the storage requirements. Furthermore, it is necessary to compute each eigen pair to a very high degree of accuracy, to prevent severe roundoff errors.

In this study none of the above two methods are used, instead, the following more efficient measure is adopted. When eigenvalues are needed for the very first time, they are calculated using the method of subspace iteration in conjunction with Jacobi diagonalization. For subsequent calculations the eigenvalue derivative information can be used since it permits the use of a Taylor series expansion to predict the approximate values of the new eigenvalues at the new design point. These approximate eigenvalues are then used to shift the stiffness matrix. Inverse iteration on this shifted matrix yields the required eigenvalues. This method preserves the skyline structure of the mass/stiffness matrices. Also one can calculate any isolated

eigenvalues without having to compute all the unnecessary intermediate eigenvalues.

Computation of the 1st, 3rd and 8th frequencies using this method is about 12 times faster as compared to the method described in (a) above. Secondly, in the case when all 8 eigenvalues are needed at a new design point, this method is on an average 3 times faster to the method described in (a) above.

This method however can be used only when a good estimate of the eigenvalues is available. This is the case during the optimization process, since eigenvalues and their derivatives with respect to the design variables are known, thereby permitting the use of a Taylor series expansion to estimate the eigenvalues at the new design point.

4.2.4 Constraint Deletion

During the subproblem solution only those frequency constraints that are likely to be violated are retained. To determine which constraints are likely to be violated, the constraints are first non-dimensionalized.

Typically the constraint equation can be written as

$$g_i - 1 > 0$$

where i refers to the ith constraint. A suitable set of numbers g_{ci} are then chosen such that if

$$g_i - 1 \geq g_{ci}$$

the ith constraint is deleted for every i for which the relationship holds. g_{ci} needs to be chosen very carefully. If it is chosen too large, then too many constraints are retained in the active set. On the

other hand if g_{cj} is chosen too small, too many constraints will be deleted and the solution may wander into the infeasible region. It is helpful to group the constraints into different groups (i.e., frequency constraints, constraints due to bounds on the design variables, etc.) and then specify a different constraint deletion criterion for each group. Computational experience shows that good results can be obtained by specifying g_{cj} arbitrarily to be a low value such as 0.2, and then limiting the number of constraints deleted from each group to a small number. This ensures that we delete some constraints for each subproblem and also reduces the probability of the solution wandering into the infeasible region. Using the above procedure it was found that with two frequency constraints deleted the CPU time needed for the subproblem optimization is reduced by twenty five percent.

4.2.5 Using the Hessian Calculated in the Previous Subproblem as an Initial Estimate to the Current Hessian

The VMCON algorithm uses the identity matrix as an initial approximate estimate to Hessian matrix of the Lagrange function defined by Eq. (B.1.3). The solution time for the subproblem depends on how close the initial estimate for the Hessian is to the actual Hessian at the optimal point. Intuitively it seems reasonable that the Hessian matrix of the previous optimization subproblem would be a better estimate than starting out with the identity matrix as an initial approximation to the Hessian matrix of the current subproblem. It is found that this indeed is the case. The saving of CPU time is about 50 percent, for the problem considered. Percentage saving in CPU time =

$100x(T_I - T_H)/T_H$, where T_I = 354 seconds is the CPU time on a VAX 11/780 for subproblem solution when identity matrix is used as the initial approximation, and T_H = 236 seconds on the same machine for subproblem solution when Hessian at the end of the previous subproblem solution is used as an initial approximation to the Hessian matrix of the current subproblem.

As the number of design variables changes from one subproblem to the next, only those elements of the Hessian matrix corresponding to design variables in the current problem that were also present in the previous subproblem are retained for the purposes of approximation. For those new design variables which enter the design space the elements of the Hessian matrix are assumed to be

$$\begin{aligned} A(i,j) &= 1 \quad \text{if } i = j \\ A(i,j) &= 0 \quad \text{otherwise} \end{aligned} \tag{4.2.5.1}$$

4.3 Implementation of Structural Control Calculations

To study the effect of structural optimization on structural control, IMSC is used to calculate the performance index, modal control forces, actuator forces, etc., for the unoptimized and optimized structures. Each of the above quantities depend on the structural frequencies, the initial conditions and the penalty parameters R_r (see Appendix C). The initial conditions can be specified either in the modal space directly, or alternately, they can be specified in the physical space (in terms of nodal displacements and velocities) and then

transformed to the modal space. Since the intent here is to compare the performance of an unoptimized structure with that of an optimized structure, the initial conditions are specified in terms of a loading (or external disturbance) that is the same for the unoptimized and optimized structure. In other words, deflections that would be produced by the same load are taken to be the initial conditions, in each case. It should be noted that the same nodal load vector, F, will produce different deflections (both in the modal and physical space) in the unoptimized and optimized structure. Prescribing the initial conditions in this fashion ensures that the performance of the structure when subjected to identical "external" loads is compared. In aerospace applications this is indeed a meaningful comparison. However, in earthquake type problems, it would be more meaningful perhaps to specify the initial conditions directly in terms of given deflections, for comparison purposes. If F be the given nodal load vector, applied statically, the initial modal displacement ξ_r corresponding to the rth mode is given by

$$\xi_r = \frac{x_r^T F}{\lambda_r} \tag{4.3.2}$$

where λ_r, x_r are the rth eigenvalue and corresponding eigenvector, respectively.

Table 12 defines the three nodal load vectors, identified as Load 1, Load 2, and Load 3, used to simulate certain initial conditions. Load 1 and Load 2 excite the first and second modes of the structure,

respectively, while Load 3 excites the second and fourth modes, predominantly.

4.4 Discussion of Results

The procedure outlined in this study along with the proposed efficiency measures is a viable and cost effective method for optimization of stiffened laminated composite plates. Table 9 provides the CPU time spent for each of the 22 subproblems, which were required for complete convergence to the final solution (OPT1b). The results of Table 9 show that the efficiency measures adopted, drastically reduce the solution time for the subproblem optimization, making integer programming a viable alternative in structural optimization. By adding up the entries in Table 9 it is seen that the CPU time required to obtain an integer feasible optimal solution is roughly four times that of determining the first continuous solution. It is important to note that without the efficiency measures discussed before, the CPU time requirements would have been at least twenty times those of the continuous solution.

Table 5 emphasizes the need for integer programming as opposed to obtaining an approximate solution by rounding off of a single continuous optimization problem. In all the cases considered in Table 5, the rounded off solution is infeasible, as indicated by the negative values of g_1, g_2, g_3. The quantities g_1, g_2, g_3 are the values of the normalized inequality constraints, required to be positive to ensure prescribed frequency separation. The continuous solution and the optimal solution are always feasible, as indicated by Table 5.

Intuition seems to indicate that as the number of plies is increased the effect of a single ply on the overall behavior of the plate should reduce. In other words as the number of plies is increased an absence or the presence of any one ply would not effect the plate behavior significantly. If this is true then the effect of rounding off would reduce as the number of plies is increased. An examination of Table 5 seems to indicate that this is indeed true for the designs considered. For a total of 12 plies the rounded off design experiences a maximum constraint violation of 8%. When the number of plies is increased to 18 and 24, the corresponding constraint violation reduces to 6% and 1% respectively. This suggests that there is not much to be gained by employing the costly nonlinear mixed integer programming technique to obtain the optimum solutions in the case of thick laminates with a large number of plies. Rounded off designs that can be obtained cheaply would be good enough.

Table 10 lists the final design vectors that were obtained as solutions to the structural optimiztion problems defined in Table 4. Table 11 provides the 8 lowest frequencies for each of the optimized structures listed in Table 10. Each of the frequencies is given as a ratio corresponding to the fundamental frequency of the initial design listed in Table 3. Table 11 indicates that of the various optimization schemes considered, scheme OPT1b leads to the largest increase in all the eight frequencies. It also indicates that the structural frequencies can be increased by specifying higher target frequencies. For example the target frequencies for OPT2c are higher than those for

OPT2b which are in turn higher than those of OPT2a. As a result, the structural frequencies for OPT2c are higher than those for OPT2b which are in turn higher to those of OPT2a. The target frequencies for OPT2d were specified such that only the first and third frequencies would be increased while the 2nd frequency was held fixed. Table 11 that the second frequency of the optimized structure OPT2d is the same as that of the unoptimized structure, while the first and third frequencies have increased.

To consider the impact of structural optimization on structural control the performance indices of the unoptimized structure to that of the optimized structure were compared. To get an estimate of the maximum modal control force and actuator forces the norm of these quantities at t=0 is compared. For the purpose of definition the norm of an n dimensional vector X is taken to be

$$\text{Norm of } X = (X^T X)^{1/2}$$

in this work. The performance index is an integrated measure of the controller performance. Norm of the modal control forces and the actuator forces, as defined above would give an estimate of the force and hence the size requirements. The ratios of the above quantities, namely the performance index and the modal and actuator forces, for the unoptimized structure to that of the optimized structure are taken to be a measure of the improvement achieved through structural optimization. Values greater than unity for these ratios indicate improvement while values smaller than unity indicate a deterioration in control performance.

Calculation of all the above quantities requires a knowleldge of the initial modal displacements. Tables 13a, 13b and 13c list the initial modal displacements calculated using Eq. (4.2.2) for Load 1, Load 2 and Load 3, respctively, for structures defined in Table 10. Table 14, lists the values of the performance index calculated using Eqs. (3.3.12) for the unoptimized and the optimized structures listed in Table 10. The initial conditions used are those listed in Tables 13a, 13b and 13c for various values of the penalty parameter R. The same penalty parameter is used for all the modes. The first 8 modes are used in the calculation of the performance index. Table 15 gives the ratios of the performance indices of the unoptimized structure and the optimized structures, listed in Table 14. Table 16 gives the norm of the modal control forces for the unoptimized structure and the various optimized structures. The modal control forces are calculated using Eqs. (C.2.3-C.2.8) of Appendix C. Table 17 shows the ratios of the modal control forces for the unoptimized structure and the various optimized structures. The actuator forces depend on the placement of the actuators and Table 18 shows the actuator forces for two possible sets of actuator locations. Table 19 provides the ratios of the norms of the actuator forces for the unoptimized structure to the corresponding norms of the optimized structure for each of the two cases considered in Table 18.

Figure 6 shows a plot of the performance index of the first mode as a function of the first frequency. In IMSC the overall performance index J, given by Eq. (C.2.1) is minimized by minimizing each modal

performance index J_r independently. This indicates that to reduce the value of J, given by Eq. (C.2.1), it is necessary to increase each structural frequency. Increase in structural frequencies is achieved through structural optimization.

Inspection of Table 15 indicates that the ratios of the performance indices J of the unoptimized structure to that of the optimized structure are independent of the penalty parameter R. However, the ratios are a function of the initial conditions and the structural frequencies. The gain in control performance, as measured by the ratio of the performance index of the unoptimized structure to that of the optimized structure, increases as the structural frequencies are increased. From Table 11 it is seen that the optimization scheme OPT1b has the largest increase in all the seven frequencies considered. An examination of Table 15 indicates, that this optimization scheme (OPT1b) does indeed experience the maximum gain in control performance.

Initial conditions, also determine the gains achieved in control performance. In Table 15, Load 1 corresponds to initial conditions whereby the lowest structural vibration mode is excited, whereas Load 2 and Load 3 correspond to initial conditions wherein higher modes are excited. This fact can be ascertained by comparing corresponding columns of Tables 13a, 13b, and 13c. Further inspection of Table 15, indicates that the gain in control performance, due to structural optimization, is the largest for Load 1 and smallest for Load 3, for all the structures OPT1b, OPT2a, OPT2b and OPT2c. This is due to the fact, that for all these optimized structures the lower frequencies experience

a larger percentage increase as compared to the higher frequencies. For example, in the optimization scheme OPT1b (see Table 11) the fundamental frequency increases by 225%, while the seventh frequency increases by only 60%. As a result, for these structures (OPT1b, OPT2a, OPT2b, OPT2c) the gain in the control performance due to optimization, for vibration suppression is more for low frequency disturbances and less for high frequency disturbances.

To investigate the above point further, the target frequencies for the optimization scheme OPT2d were specified such that the first and third frequencies would be significantly increased while holding the second frequency fixed (see Tables 6,11). An examination of Table 15 (OPT2d) indicates that the gain in control performance for initial conditions as specified by Load 2, where the second frequency is excited predominantly, is less than those for Load 1 and Load 3.

Tables 16 and 17 show similar results for the norms of the modal control forces. Table 17 indicates that the ratio of the norms of the modal control forces of the unoptimized structure to that of the optimized structure are independent of the penalty parameter R, for the cases considered. An increase in the structural frequencies leads to a corresponding decrease in the norm of the modal control force. In fact if the ratios of the norms of the modal control vector of the unoptimized structure to that of the optimized structure are taken to be a measure of improvement in control performance due to optimization, then Table 17 indicates that similar conclusions to those drawn above from Table 15, for the performance index can also be arrived at for the

modal control vector. However, there is a difference for the case OPT2d, wherein the norm of the modal control force corresponding to the initial conditions Load 2 does not reduce as a result of optimization. For initial conditions corresponding to Load 1 and Load 3 there is, however, a definite reduction in the norm of the modal control forces. One can therefore say that there is no gain in control performance corresponding to initial conditions Load 2 due to optimization. It should be noted that in the scheme OPT2d the second frequency is held fixed, while frequencies 1 and 3 are increased.

In the IMSC implementation of optimal control, the synthesis of the actuator forces from the modal control forces is a separate design step. Table 18 shows how the actuator forces can be different for a given modal control vector, depending on the actuator locations. Inspection of Table 19 indicates that substantial reduction in actuator forces can be achieved through structural optimization. However, unlike the results of Table 15 and Table 17, the ratios depend on the penalty parameter R.

CHAPTER 5

CONCLUSION

It is shown that integer programming is a viable alternative to structural optimization as opposed to the conventional practice of rounding off, when some of the design variables are restricted to integer values. Rounding off of the continuous solution leads to infeasible designs in some cases. As the number of plies is increased the effect of the presence or absence of any singly ply is reduced, thereby reducing the effect of round off. For example when the total number of plies is twelve the maximum constraint violation for the rounded off solution is 8%. When the number of plies is increased to 18 and 24, the corresponding constraint violation reduces to 6% and 1% respectively. This suggests that there is not much to be gained by employing the costly nonlinear mixed integer programming technique to obtain the optimum solutions in the case of thick laminates with a large number of plies. Rounded off designs that can be obtained cheaply would be good enough.

Several subproblem optimizations are necessary to obtain an integer feasible optimal solution. A number of measures need to be taken to reduce the CPU time required. Some of these measures include deletion of integer design variables from the subproblem design space, storing of integration results needed to assemble element mass and stiffness matrices, fast recalculation of structural frequencies, constraint deletion and use of previous Hessian matrix as an initial guess. Each ofthese measures lead to an acceleration of the subproblem optimization

and reduce the CPU time requirements. These measures were found to be both effective and necessary, to solve the integer programming problem in a reasonable amount of time.

It has been shown that sufficient improvement in control performance can be achieved through structural optimization. The ratios of the performance index, the norm of the modal control vectors and the norm of the actuator forces of the unoptimized structure to that of the optimized structure have each been considered, for various values of the penalty parameter as well as different initial conditions. In each case, the control performance of the optimized structure, as measured by the above ratios, has been found to be superior to that of the unoptimized structure. It was also observed that the above mentioned ratios for the performance index and the modal control forces are independent of the penalty parameter R, for the cases considered. The ratios of the actuator forces, however, were found to be a function of the penalty parameter R.

The initial conditions were found to determine the amount of improvement due to optimization, in the control performance, as measured by the above ratios. When the first and the third frequencies were increased and the second frequency kept fixed, it was found that if the initial conditions specified were such that the second mode was excited than the improvement in control performance was marginal. For the same structure, when the initial conditions were such that modes other than the second were excited, there was a substantial improvement in the control performance.

An increase in structural frequencies correspond to an increase in structurl stiffness. To attain an improvement in control performance it is therefore necessary to increase the stiffness of the structure that is to be controlled. This work shows the precise nature of the increase in stiffness that one must seek in order to improve the control performance. Any arbitrary increase in structural stiffness does not necessarily improve the control performance as shown above. Improvements in control performance can be achieved only through increases in structural stiffness that are commensurate with the specified initial conditions of the problem.

REFERENCES

1. Hale, A. L., Lisowski, R. J., and Dahl, W. E., "Optimizing Both the Structure and the Control of Maneuvering Flexible Spacecraft," presented as Paper No. 83-377, at the AAS/AIAA Astrodynamics Specialist Conference, Lake Placid, NY, August 22-25, 1983.

2. Hale, A. L., and Lisowski, R. J., "Optimal Simultaneous Structural and Control Design of Maneuvering Flexible Spacecraft," presented at the Fourth VPI&SU/AIAA Symposium on Dynamics & Control of Large Space Structures, Blacksburg, VA, June 6-8, 1983.

3. Messac, A., and Turner, J., "Dual Structural Control Optimization of Large Space Structures," NASA Symposium on Recent Experiences in Multidisciplinary Analysis and Optimization.

4. Khot, N. S, Venkayya, V. B., and Eastep, F. E., "Structural Modifications to Reduce the LOS Error in Large Space Structures," (84-0997-CP) AIAA/ASME/ASCE/AHS 25th Structures, Structural Dynamics & Materials Conference, Palm Springs, CA, May 14-16, 1984.

5. Khot, N. S., Venkayya, V. B., and Eastep, F. E., "Structural Modification of Large Flexible Structures to Improve Controllability," (84-1906) Proceedings of the AIAA Guidance & Control Conference, Seattle, WA, August 1984.

6. Bodden, D. S., and Junkins, J. L., "Eigenvalue Optimization Algorithms for Structural/Controller Design Iterations," presented in the 1984 American Control Conference, June 6-8, 1984, San Diego, CA.

7. Junkins, J. L., Bodden, D. S., and Turner, J. D., "A Unified Approach to Structure and Control System Design Iterations," presented to the Fourth International Conference on Applied Numerical Modelling, Tainan, Taiwan, Dec. 27-29, 1984.

8. Chun, H. M., "Optimal Distributed Control of a Flexible Spacecraft During a Large Angle Rotational Maneuver," MIT MS Thesis, June 1982, Cambridge, MA.

9. Salama, M., Hamidi, M., and Demsetz, L., "Optimization of Controlled Structures," presented at the Jet Propulsion Workshop on Identification & Control of Flexible Space Structures, San Diego, CA, June 4-6, 1984.

10. Hale, A. L., "Integrated Structural/Control Synthesis via Set-Theoretical Methods," Proceedings of the AIAA/ASME/ASCE/AHS 26th Struct., Struct. Dyn., & Matl. Conf., Part 2, Orlando, FL, April 15-17, 1985, pp. 636-641.

11. Haftka, R. T., Martinovic, Z. N., and Hallauer, W. L., Jr., "Sensitivity of Optimized Control Systems to Minor Structural Modifications," 26th Struct., Struct. Dyn., & Matl. Conf., Part 2, Orlando, FL, April 15-17, 1985, pp. 642-650.

12. Haftka, R. T., Martinovic, Z. N., and Hallauer, W. L., Jr., "Enhanced Vibration Controllability by Minor Structural Modification," AIAA Paper No. 84-1036-CP, presented at the AIAA Dynamics Specialist Conference, Palm Springs, CA, May 1984.

13. Lamberson, S. E., and Yang, T. Y., "Optimization Using Lattice Plate Finite Elements for Feedback Control of Space Structures," 26th Struct., Struct. Dyn., & Matl. Conf., Part 2, Orlando, FL, April 15-17, 1985, pp. 642-650.

14. Dantzig, G. B., Fulkerson, D. R., and Johnson, S. M., "Solution of Large Scale Travelling Salesman Problem," Oper. Res. 2, 393-410 (1954).

15. Markovitz, H. M., and Manne, A. S., "On the Solution of Discrete Programming Problems," 1957, Econometrica 25, 84-110.

16. Dantzig, G. B., "Notes on Solving Linear Problems in Integers," 1959, Nav. Res. Logist, Quarterly, 75-76.

17. Gomory, R. E., "Outline of an Algorithm for Integer Solutions to Linear Problems," 1958, Bull. Amer. Math. Soc. 64, 275-278.

18. Gomory, R. E., "All Integer Programming Algorithm," 1960, RC-189, IBM, Yorktown Heights, NY.

19. Gomory, R. E., "An Algorithm for the Mixed Integer Problem," 1960, RM-2597, RAND Corp., Santa Monica, CA.

20. Glover, F., "A Bound Escalation Method for the Solution of Integer Linear Programs," 1965, Cah. Cent. Etud. Rech. Operationelle 6, 131-168.

21. Young, R. D. (1971), "Hypercylindrically Deduced Cuts in 0-1 Integer Programming," 1971, Oper. Res. 19, 1393-1405.

22. Balas, E., "Intersection Cuts - A New Type of Cutting Planes Method for Integer Programming," 1971, Oper. Res. 19, 19-39.

23. Glover, F., "Convexity Cut and Cut Search," 1971, Oper. Res. 21, 123-134.

24. Ben-Israel, A. and Charnes, A., "On Some Problems in Diophantine Programming," 1962, Cah. Cent. Etud. Rech. Operationelle 4, 215-280.

25. Young, R. D., "A Primal (all integer) Integer Programming Algorithm," 1965, J. Res. Nat. Bur. Stand. Sect. B, 69, 213-250.

26. Young, R. D., "A Simplified Primal (all integer) Inter Programming Algorithm," 1968, Oper. Res. 16, 750-782.

27. Glover, F., "A New Foundation for a Simplified Primal Integer Programming Algorithm," 1968, Oper. Res. 16, 727-740.

28. Bertier, P., and Roy, B., "Une Procedure de Resolution pour une Classe de Problemes Pouvant avoir un Charactere Combinatoire," 1965, Intl. Comput. Cent. Bull. 4, 19-28 (Transl. by W. S. Jewell, ORC Rep. 67-34, Univ. of Calif., Berkeley).

29. Balas, E., "A Note on the Branch and Bound Principle," 1968, Oper. Res. 16, 442-445; errata Oper. Res. 16, 886.

30. Mitten, L. G., "Branch and Bound Methods: General Formulations and Properties," 1970, Oper. Res. 18, 24-34.

31. Land, A. H., and Doig, A. G., "An Automatic Method for Solving Discrete Programming Problems," 1960, Econometrica 28, 497-520.

32. Dakin, R. J., "A Tree Search Algorithm for Mixed Integer Programming Problems," Computer Journal, Vol. 8, No. 3, 1965, pp. 250-255.

33. Gupta, O. K., "Branch and Bound Experiments in Nonlinear Integer Programming," Ph.D. Thesis, Purdue Univ., 1980.

34. Gupta, O., and Ravindran, A., "Nonlinear Integer Programming and Discrete Optimization," ASME Transactions, Journal of Mechanisms, Transmissions, & Automation in Design, Vol. 105, No. 2, June 1983.

35. Schmit, L. A., and Fleury, C., "Discrete-continuous Variable Structural Synthesis Using Dual Methods," AIAA J., Vol. 18, No. 12, Dec. 1980.

36. Imai, K., "Structural Optimization by Material Selection," Information Processing Center, Kajima Corp., Dec. 1979.

37. Hua, H. M., "Optimization for Structures of Discrete-Size Elements," Computers & Structures, Vol. 17, No. 3, pp. 327-333, 1983.

38. Johnson, R. C., "Rigid-Plastic Minimum Weight Plane Frame Design Using Hot Rolled Shapes," Proceedings of the Intl. Symposium on Optimum Structural Design, Tucson, AZ, Oct. 1981.

39. Gisvold, K. M., "A Method for Nonlinear Mixed-Integer Programming and Its Application to Design Problems," presented at the Vibrations & International Design Automation Conference, Toronto, Canada, Sept. 8-10, 1971, ASME.

40. Templeman, A. B., and Yates, D. F., "A Segmented Method for the Discrete Optimum Design of Structures," Engineering Optimization, 1983, Vol. 6, pp. 145-155, Gordon & Breach Science Publishers, Inc.

41. Greenberg, H. J., and Prager, W., "On Limit Design of Beams and Frames," Technical Report, Brown Univ., Office of Naval Research, Contract N7Onr-35806, Oct. 1949.

42. Livesley, R. K., "The Automatic Design of Structural Frames," Quart. J. Mech. Appl. Math., 9, Part 3 (1956).

43. Schmit, L. A., "Structural Design by Systematic Synthesis," Proc. of 2nd National Conf. on Electronic Computation, ASCE, 1960, pp. 105-132.

44. Moses, F., "Optimum Standard Design Using Mathematical Programming," J. of the Structural Div., ASCE, Vol. 90, No. ST6, Dec. 1964, pp. 89-104.

45. Venkayya, V., "Design of Optimum Structures," Computers & Structures, 1, No. 1/2, 265-309 (1971).

46. Prager, W., and Marcal, P., "Optimality Criteria in Structural Design," AFFDL-TR-70-166, May 1971.

47. Taylor, J., "Optimal Design of Structural Systems" An Energy Formulation," AIAA J., 7, pp. 1404-1406 (1969).

48. Kicher, T. P., "Optimum Design Versus Fully Stressed," Proc. ASCE Journal of Struct. Div., Vol. 92, No. ST6, 1966.

49. Fleury, C., and Sander, G., "Relationships Between Optimality Criteria and Mathematical Programming in Structural Optimization," Proc. Symp. Applications for Computer Meth. in Engrg. (Ed. C. Wellford, Jr.), Univ. of Southern California, 507-520 (1977).

50. Fleury, C., and Schmit, L. A., "Prime and Dual Methods in Structural Optimization," Journal of the Structural Division, ASCE, Vol. 106, No. ST5, Proc. Paper 15431, May 1980, pp. 1117-1133.

51. Schmit, L. A., and Farshi, B., "Some Approximation Concepts for Structural Synthesis," AIAA Paper No. 73-341, AIAA/ASME/SAE 14th Structures, Structural Dynamics & Materials Conference, Williamsburg, VA, March 1973.

52. Haftka, R. T., and Yates, E. C., Jr., "On Repetitive Flutter Calculations in Structural Design," AIAA 12 Aerospace Sciences Meeting, Washington, D.C., January 1974, Paper No. 74-141.

53. Haftka, R. T., and Yates, E. C., Jr., "Repetitive Flutter Calculations in Structural Design," Journal of Aircraft, Vol. 13, pp. 454-461, 1976.

54. Rosen, J. B., "The Gradient Projection Method of Linear Programming Part 1: Linear Constraints," SIAM J. 8, 181-217, 1960.

55. Rosen, J. B., "The Gradient Projection Method of Linear Programming Part 1: Nonlinear Constraints," SIAM J. 9, 541-532, 1961.

56. Zoutendijk, G., "Methods of Feasible Directions," Elsevier, Amsterdam, 1960.

57. Vanderplaats, G. N., "CONMIN - A Fortran Program for Constrained Function Minimization: User's Manual," NASA TM X-62282, 1973.

58. Vanderplaats, G. N., Sugimoto, H., and Sprague, C. M., "ADS-1: A New General Purpose Optimization Program," AIAA Paper No. 83-0831, presented at the AIAA/ASME/ASCE/AHS 24th Structures, Structural Dynamics & Materials Conf., Lake Tahoe, CA, May 1983.

59. Haftka, R. T., and Kamat, M. P., "Elements of Structural Optimization," Martinus Nojhoff Publishers, 1985.

60. Kavlie, D., and Moe, J., "Automated Design of Frame Structures," ASCE J. Struc. Div., 33-62, 1971.

61. Haftka, R. T., and Starnes, J. H., Jr., "Applications of a Quadratic Extended Penalty Function to Structural Optimization," AIAA J. 14, 718-724, 1976.

62. Prasad, B., "A Class of Generalized Variable Penalty Methods for Nonlinear Programming," J. Optimization Theory & Applications 35, 159-182, 1981.

63. Fiacco, A. V., and McCormick, G. P., "Nonlinear Programming: Sequential Unconstrained Minimization Techniques," Wiley, NY, 1969.

64. Miura, H., and Schmit, L. A., Jr., "NEWSUMT - A Fortran Program for Inequality Constrained Function Minimization - User's Guide," NASA CR-159070, June 1979.

65. Falk, J. E., "Lagrange Multipliers and Nonlinear Programming," J. Math. Anal. Appl. 19, 141-159, 1967.

66. Powell, M. J. D., "A Fast Algorithm for Nonlinearly Constrained Optimization Calculations," in Proc. of the 1977 Dundee Conf. on Numerical Analysis, Lecture Note in Mathematics, Springer-Verlag, 1978.

67. Fleury, C., "Structural Weight Optimization by Dual Methods of Convex Programming," Intl. J. Num. Meth. Engrg., 14, 1761-1783, 1979.

68. Fleury, C., and Schmit, L. A., "ACCESS 3-APPROXIMATION Concepts Code for Efficient Structural Synthesis - User's Guide," NASA CR-159260, Sept. 1980.

69. Cilley, F. H., "The Exact Design of Statically Determinate Frameworks, and Exposition of Its Possibility, But Futility," Trans. ASCE 43, 353-407, 1900.

70. Khot, N. S., Venkayya, V. B., and Berke, L., "Optimum Design of Composite Structures with Stress and Displacement Constraints," AIAA Journal, Vol. 14, Feb. 1976, pp. 131-137.

71. Khot, N. S., "Optimal Design of a Structure for System Stability for a Specified Eigenvalue Distribution," Proceedings, International Symposium on Optimum Structural Design, Tucson, AZ, pp. 1-3, Oct. 1981.

72. Nshanian, Y. S., and Pappas, M., "Optimal Design of Laminated Composite Plates," NJIT Report NV-16, Dec. 1981.

73. Hirano, Y., "Optimal Design of Laminated Plates Under Axial Compression," AIAA Journal, Vol. 17, Sept. 1979, pp. 1017-1018.

74. Nshanian, Y. S., and Pappas, M., "Optimal Laminated Composite Shells for Buckling and Vibration," AIAA Journal, Vol. 21, March 1983, pp. 430-437.

75. Bryson, A. E., and Ho, Y. C., "Applied Control Theory," Blaisdel Publishing Co., Waltham, MA, 1969.

76. Florentin, J. J., "Optimal Control of Continuous-Time Markow Stochastic Systems," Journal of Electro. Contr., IEEE, Vol. 10, pp. 473-488.

77. Kalman, R. E., and Bucy, R. S., "New Results in Linear Filtering and Prediction Theory," Journal of Basic Engineering, Transactions, American Society of Mechanical Engineering, Vol. 83, 1961.

78. Tse, E., "On the Optimal Control of Stochastic Linear Systems," IEEE Transactions on Automatic Control, Vol. AC-16, No. 6, 1971, pp. 776-785.

79. Wonhan, W. M., "On the Separation Theorem of Stochastic Control," Society for Industrial & Applied Mathematics Journal for Control, Vol. 6, No. 2, 1968, pp. 313-326.

80. Blackburn, T. R., and Vaughan, D. T., "Application of Linear Optimal Control Filtering Theory to the Saturn V Launch Vehicle," IEEE Transactions on Automatic Control, Dec. 1971, pp. 799-806.

81. Luh, J. Y. S., and Lukas, M. P., "Suboptimal Closed-Loop Controller Design for Minimum Probability of Inequality Constraints Violation," IEEE Transactions on Automatic Control, Oct. 1969, pp. 449-457.

82. Swaim, R. L., "Control System Synthesis for a Launch Vehicle with Severe Mode Interaction," IEEE Transactions on Automatic Control, Vol. AC-16, No. 6, 1971, pp. 776-785.

83. Bender, E. K., "Optimum Linear Preview Control with Application to Vehicle Suspension," Journal of Basic Engineering, Transactions, ASME, Vol. 90, No. 2, 1968, pp. 213-221.

84. Karnopp, D. C., "Applications of Random Process Theory to the Design & Testing of Ground Vehicles," Transportation Research, Vol. 2, 1968, pp. 269-278.

85. Sevin, E., and Pilkey, W. D., "Optimum Shock and Vibration Isolation," SVM-6, The Shock & Vibration Information, U.S. Dept. of Defense, Washington, D.C., 1971.

86. Meirovitch, L., and Oz, H., "Active Control of Structures by Modal Synthesis," Structural Control, H. H. E. Leipholz (ed.), North Holland Publishing Co. & SM Publications @ IUTAM, 1980.

87. Meirovitch, L., Baruh, H., and Oz, H., "A Comparison of Control Techniques for Large Flexible Systems," AIAA Journal of Guidance, Control & Dynamics, Vol. 6, Nov. 4, July-Aug. 1983, pp. 302-310.

88. VanLandingham, H. F., Caglayan, A. K., and Floyd, J. B., "Approximation Techniques for Optimal Modal Control of Flexible Systems," Proceedings of the 3rd VPI&SU/AIAA Symposium held in Blacksburg, VA, June 15-17, 1981.

89. Baruh, H., and Meirovitch, L., "On the Placement in the Control of Distributed-Parameter Systems," Proceedings of the AIAA Dynamics Specialist Conference, AIAA, New York, 1981, pp. 611-620.

90. Kamat, M. P., "Active Control of Structures in Nonlinear Response," Optimization Issues in the Design & Control of Large Space Structures, Ed. M. P. Kamat, Proceedings of the ASCE Denver Convention, April 1985, pp. 46-59.

91. Tripathy, S. S., "Optimization Using Conjugate Gradient Methods," IEEE Transactions on Automatic Control, April 1970, pp. 268-270.

92. Herrick, D. C., Canavin, J. R., and Strunce, R. R., "An Experimental Investigation of Modern Control," AIAA Paper 79-0199, 17th AIAA Aerospace Sciences Meeting, New Orleans, Jan. 15-17, 1979.

93. Roorda, J., "Experiments in Feedback Control of Structures," H. H. E. Leipholz, ed., Structural Control Proc. of the IUTAM Symposium on Structural Control held at the Univ. of Waterloo, Ontario, Canada, pp. 629-661, June 4-7, 1979, North Holland Publications, 1980.

94. Stroud, R. C., Hamma, G. A., Smith, S., and Lyons, M. G., "Developments Toward Active Control of Space Structure," SAE Paper 801234, SAE Aerospace Meeting, Los Angeles, Oct. 13-16, 1980.

95. Rockwell, T. H., and Lawther, J. M., "Theoretical and Experimental Dampers," Journal of the Acoustical Society of America, 36(8), 1507-1515, 1964.

96. Knyazev, A. S., and Tartakovskii, B. D., "Vibrational Frequency Characteristics of Bars Constrained by Electromechanical Feedback," Soviet Physics-Acoustics, 12(1), 36-41, 1966.

97. Swigert, C. J., and Forward, R. L., "Electronic Damping of Orthogonal Bending Modes in a Cylindrical Mast - Theory and Experiment," Journal of Spacecraft & Rockets, 18(1), 5-17, 1981.

98. Hallauer, W. L., Skidmore, G. R., and Mesquita, L. C., "Experimental Theoretical Study of Active Vibration Control," 1st International Modal Analysis Conference, Nov. 8-10, 1982, Orlando, FL.

99. Meirovitch, L., Baruh, H., Montgomery, R. C., and Williams, J. P., "Nonlinear Natural Control of an Experimental Beam," AIAA J. of Guidance, Control & Dynamics, Vol. 7, No. 4, July-August 1984, pp. 437-442.

100. Little, J. D. C., Murthy, K. G., Sweeney, D. W., and Karel, C., "An Algorithm for the Travelling Salesman Problem," Oper. Res. 11, pp. 979-989, 1960.

101. Hamdy, A. T., "Integer Programming," 1975, Academic Press, p. 171.

102. Reddy, J. N., "Simple Finite Elements with Relaxed Continuity for Nonlinear Analysis of Plates," Proc. 3rd Intl. Conf. in Australia on Finite Element Methods, Univ. of New South Wales, Syndey, July 2-6, 1979.

103. Meirovitch, L., and Silverberg, L. M., "Control of Structures Subjected to Seismic Excitation," Journal of Engng. Mech., Vol. 109, No. 2, April 1983, pp. 604-618.

104. Reddy, J. N., "An Introduction to the Finite Element Method," McGraw Hill Book Co., 1984.

105. Biggs, M. C., "Constrained Minimization Using Recursive Quadratic Programming; Some Alternative Problem Formulations" in Towards Global Optimization, eds. L. C. W. Dixon and G. P. Szego, North Holland Publishing Co. (Amsterdam).

106. Fletcher, R., "An Ideal Penalty Function for Constrained Optimization," J. Inst. Maths. Applics., 1975, Vol. 15, pp. 319-342.

107. Han, S. P., "Superlinearly Convergent Variable Metric Algorithms for General Nonlinear Programming Problems," Mathematical Programming, Vol. 11, pp. 263-282.

108. Reissner, E., "On Transverse Bending of Plates, Including the Effect of Transverse Shear Deformations," Intl. J. Sol. Struc. 11, pp. 569-573, 1975.

109. Mindlin, R. D., "Influence of Rotary Inertia and Shear on Flexural Motions of Isoptropic, Elastic Plates," J. Applied Mechanics 18, pp. 31-38, 1951.

110. Stavsky, Y., "On the Theory of Symmetrically Heterogeneous Plates Having the Same Thickness Variation of the Elastic Moduli" in Topics in Appl. Mech. (eds. D. Abir, F. Ollendorf and M. Reiner), American Elsevier, NY, 1965.

111. Yang, P. C., Norris, C. H., and Stavsky, Y., "Elastic Wave Propagation in Heterogeneous Plates," Intl. J. of Solids & Structures, Vol. 2, pp. 665-684, October 1966.

112. Sun, C. T., and Whitney, J. M., "Theories for the Dynamic Response of Laminated Plates," AIAA J., 11, 178-183 (1973).

113. Srinivas, S., and Rao, A. K., "Bending, Vibration, and Buckling of Simply Supported Thick Orthothropic Rectangular Plates and Laminates," Intl. J. Sol. Struc., 6, pp. 1463-1481, 1970.

114. Reddy, J. N., "Comparison of Closed Form and Finite-Element Solutions for Bending and Free Vibrations of Layered Composite Rectangular Plates," Rep. OU-AMNE-79-20, School of Aerospace, Mechanical, & Nuclear Engineering, Univ. of Oklahoma, Norman, OK.

115. Whitney, J. M., "The Effect of Transverse Shear Deformation on the Bending of Laminated Plates," J. Comp. Materials 3, pp. 534-547, 1969.

116. Bathe, K. J., "Finite Element Procedures in Engineering Analysis," Prentice Hall, Inc., Englewood Cliffs, NJ.

Appendix A

A.1 Outline of the Branch and Bound Algorithm

The procedure adopted for solving the nonlinear mixed integer programming (NMIP) problem is an extension of the procedure suggested by Dakin [32]. This procedure is applicable to both linear as well as nonlinear mixed integer programming problems. The procedure consists of a systematic search of continuous solutions in which certain variables are successively forced to take on integral values; the logical structure of the set of solutions is that of a tree. The algorithm starts by finding a solution to the continuous problem wherein the integrality requirements are relaxed. If this solution is integral, then it is the optimal solution to the given discrete problem. If the solution is nonintegral then at least one integer variable, say x_k, is nonintegral, and takes the value, say b_k which can be divided into integral and fractional parts [b] and f respectively as

$$b_k = [b] + f \tag{A.1.1}$$

where [b] is integral and $0 < f < 1$. If x_k has to take an integer value then either one of the following two conditions must be satisfied.

$$x_k \leq [b] \text{ or} \tag{A.1.2}$$

$$x_k \geq [b] + 1 \tag{A.1.3}$$

This leads to two subproblems each satisfying one of the above conditions.

Subproblem (1):

$$\text{Minimize } f(x),\ x = (x_1, x_2, \ldots, x_n)^t \tag{A.1.4}$$

$$\text{Subject to } h_i(x) = 0 \quad i = 1,2,\ldots,n_e$$

$$g_j(x) \geq 0 \quad j = 1,2,\ldots,n_g$$

$$x_k \leq [b]$$

Subproblem (2):

$$\text{Minimize } f(x),\ x = (x_1, x_2, \ldots, x_n)^t \tag{A.1.5}$$

$$\text{Subject to } h_i(x) = 0 \quad i = 1,2,\ldots,n_e$$

$$g_j(x) \geq 0 \quad j = 1,2,\ldots,n_g$$

$$x_k \geq [b] + 1$$

In the subproblems, the integrality requirement on the design variables has been removed. Furtheremore, the two subproblems have removed the space $[b] < x_k < [b] + 1$ from the feasile region as this space is not allowable for an integral solution. It should also be noted that none of the integer feasible solutions have been eliminated. Each of these subproblems is then solved again as a continuous problem and the information regarding the optimal solution is stored at a corresponding node. A node stores the optimal solution and the corresponding value of the objective function, and also the lower and upper bounds on the design variables.

The foregoing procedure of branching and solving a sequence of continuos problems is continued until a feasible integer solution to one of the continuous problems is found. This integer feasible solution becomes an upper bound on the objective function. At this point, all nodes that have a value of the objective function higher than the upper

bound are eliminated from further consideration, and the corresponding nodes are said to be fathomed.

The procedure of branching and fathoming is repeated for each of the unfathomed nodes. When a feasible integer solution is found, and the value of the objective function is less than the upper bound to date, it becomes the new upper bound on the objective function. A node is fathomed (i.e. no further consideration is required) in any one of the following cases.

1 The continuous solution is a feasible integer solution.

2. The continuous solution is infeasible.

3. The optimal value (of the continuous problem) is higher than the current upper bound.

The search for the optimal solution terminates when all nodes are fathomed. The current best integer solution gives the optimal solution to the given discrete optimization problem. The work of Gupta and Ravindran [33], [34] formed the basis for the development of a code for the NMIP problem of this study.

Appendix B

B.1 Outline of the VMCON Algorithm for the Solution of the Continuous Subproblems

The VMCON algorithm described here is based amongst others on the work of Powell [66], Biggs [105], Fletcher [106] and Han [107].

This algorithm calculates the least value of a real valued function subject to equality and inequality constraints by using a variable metric method for constrained optimization. Consider the problem

$$\text{Minimize } f(x);\ x = (x_1, x_2, \ldots, x_n)^t \tag{B.1.1}$$

subject to $h_i(x) = 0 \quad i = 1,2,\ldots,n_e$

$$g_j(x) \geq 0 \quad j = 1,2,\ldots,n_g \tag{B.1.2}$$

Assume that at the i^{th} iteration the design point is x^i and a search direction S is sought. This search direction S is found from the solution of the following quadratic programming problem:

Minimize the quadratic approximation of f along S

$$Q(x) = f(x) + S^T G(x^i) + \frac{1}{2} S^T A(x^i, \Lambda^i) S \tag{B.1.3}$$

subject to the linearized constraints

$$\begin{aligned} h_j(x^i) + S^T \nabla h_j(x^i) &= 0 \quad j = 1,2,\ldots,n_e \\ g_k(x^i) + S^T \nabla g_k(x^i) &\geq 0 \quad k = 1,2,\ldots,n_g \end{aligned} \tag{B.1.4}$$

where $G(x^i)$ is the gradient of the objective function f, Λ^i are the Lagrange multipliers. The matrix A in Eq. (B.1.3) is a positive definite approximation to the Hessian of the Lagrangian function. Initiallly it is set to the identity matrix and suitably updated during each iteration to ensure its symmetry and positive definiteness. Keeping the matrix A positive definite not only helps the quadratic

programming calculation that provides S, but it also ensures that the given method is invariant under linear transformations of the variables. This makes the method insensitive to scaling of the variables and the constraint functions.

It may happen that the linearized version of the constraints in (B.1.4) are inconsistent, even though the original constraints given by Eq. (B.1.2) are consistent. To avoid this difficulty, an extra variable, ξ is introduced into the quadratic programming calculation and the constraints (B.1.4) are replaced by the conditions

$$h_j(x^i)\xi + S^T\nabla h_j(x^i) = 0 \quad j = 1,2,\ldots,n_e$$

$$g_k(x^i)\xi_k + S^T\nabla g_k(x^i) \geq 0 \quad k = 1,2,\ldots,n_g \qquad \text{(B.1.5)}$$

where ξ_k has the value

$$\xi_k = 1 \quad , \quad g_k > 0$$

$$\xi_k = \xi \quad , \quad g_k \leq 0$$

It should be noted that if $\xi_k = 1$, the corresponding constraint remains unmodified. Thus only those constraints that are not satisfied at the starting point of the iteration are modified. The constant ξ is made as large as possible subject to the condition $0 \leq \xi \leq 1$. Any freedom that remains in S is used to minimize the quadratic objective function (B.1.3).

The matrix A is updated using the BFGS (Broyden-Fletcher-Goldforb-Shanno) update.

$$A_{new} = A - \frac{A\Delta x(\Delta x)^T A}{(\Delta x)^T A \Delta x} + \frac{\nabla L(\nabla L)^T}{(\Delta x)^T \Delta x} \tag{B.1.6}$$

where

$$\Delta x = x^{i+1} - x^i \tag{B.1.7}$$

$$\nabla L = \nabla_x \ell(x^i, \Lambda^{i+1}) - \nabla_x \ell(x^i, \Lambda^i) \tag{B.1.8}$$

where ℓ is the Lagrangian function and $\nabla_x \ell$ denotes the gradient of the Lagrangian with respect to x. To guarantee the positive-definiteness of A, ∇L is modified if

$\Delta x^T \nabla L < 0.2(\Delta x)^T A \Delta x$ and replaced by

$$\nabla L' = \theta \nabla L + (1 - \theta) A \Delta x \tag{B.1.9}$$

where

$$\theta = \frac{0.8(\Delta x)^T A \Delta x}{(\Delta x)^T A \Delta x - (\Delta x)^T \nabla L} \tag{B.1.10}$$

The solution of the quadratic programming yields S and Λ^{i+1}. We then have the new iterate given by

$$x^{i+1} = x^i + \alpha S \tag{B.1.11}$$

where α is found by minimizing the function

$$\psi(\alpha) = f(\alpha) + \Sigma \mu_j |h_j(x)| + \Sigma \mu_j |\min[0, g_j(x)]| \tag{B.1.12}$$

$\mu_j = |\Lambda_j|$ for the 1st iteration

$$\text{and } \mu_j = \max\left[|\Lambda_j^i|,\ 0.5(\mu_j^{i-1} + |\Lambda_j^{i+1}|)\right] \qquad \text{(B.1.13)}$$

for subsequent iterations with the superscript i denoting the i^{th} iteration.

The summation in (B.1.12) is carried over all the equality constraints h_j ($j = 1,2,\ldots,n_e$) and all the inequality constraints g_k ($k = 1,2,\ldots,n_g$)

It is to be noted that $\psi(\alpha)$ as defined in (B.1.12) has a first derivative discontinuity. Hence one cannot minimize $\psi(\alpha)$ by algorithms that rely on the continuity of first derivative.

The procedure adopted for choosing α is as follows. A sequence α_k ($k = 0.1,2,\ldots$) is built such that $\alpha_0 = 1$. A quadratic approximation to ψ, say ψ_k is made defined by the equations

$$\psi_k(0) = \psi(0)$$

$$\psi_k'(0) = \psi'(0)$$

$$\psi_k(\alpha_{k-1}) = \psi(\alpha_{k-1}) \qquad \text{(B.1.14)}$$

α_k is then chosen to be the greater of $0.1(\alpha_{k-1})$ and the value of α that minimizes $\psi_k(\alpha)$.

For each term in the sequence the following condition is tested.

$$\psi(\alpha_k) \leq \psi(0) + 0.1\ \alpha_k \psi'(0) \qquad (B.1.15)$$

The step length α is set to α_k as soon as this inequality is satisfied.

Appendix C

INDEPENDENT MODAL SPACE CONTROL

C.1 Equations of Motion and Modal Decomposition for Flexible Structures

In this Appendix, a concise statement of the Independent Modal Space Control (IMSC) method described in Refs. [86]-[89] is given.

Optimal control of a continuous system via IMSC is accomplished by first approximating the partial differential equation model describing the structure, by a finite set of ordinary differential equations which take the form

$$M\ddot{u}(t) + Ku(t) = F(t) \tag{C.1.1}$$

where M,K are the mass and stiffness matrices of the finite element assemblage,

$u(t)$ = vector of displacements

$F(t)$ = vector of nodal forces.

The eigenvalue problem associated with the above equation has the form

$$\omega_r^2 M x_r = K x_r \tag{C.1.2}$$

The eigenvectors are normalized to satisfy

$$x_s^T M x_r = \delta_{rs}$$

$$x_s^T K x_r = \omega_r^2 \delta_{rs} \qquad r,s = 1,2,\ldots n \tag{C.1.3}$$

wherein δ_{rs} is the Kronecker delta.

The eigenvectors can be arranged in the nxn modal matrix

$$X = [x_1\ x_2\ \ldots\ x_n] \tag{C.1.4}$$

so that Eqs. (C.1.3) can be written in the compact form

$$X^T M X = I_n;\ X^T K X = \Lambda \tag{C.1.5}$$

in which I_n = a unit matrix of order n; and Λ = the diagonal matrix of eigenvalues.

Using the linear transformation

$$u(t) = X\xi(t) \tag{C.1.6}$$

and using Eqs. (C.1.5), Eq. (C.1.1) becomes

$$\ddot{\xi} + \Lambda\xi = Z_c \tag{C.1.7}$$

where

$$Z_c = X^T F \tag{C.1.8}$$

is the nodal control vector.

Equation (C.1.7) represents a set of n modal equations of the form

$$\ddot{\xi}_r + \omega_r^2 \xi_r = Z_{cr} \qquad r = 1,2,\ldots,n \tag{C.1.9}$$

In Independent Modal Space Control (IMSC), Z_{cr} depends on ξ_r and $\dot{\xi}_r$ alone

$$Z_{cr} = Z_{cr}(\xi_r, \dot{\xi}_r) \tag{C.1.10}$$

Equations (C.1.9) are n decoupled set of equations. It follows that each mode can be controlled independently of the other modes.

C.2. Linear Optimal Control

In the IMSC technique the performance index that is to be minimized is taken in the form

$$J = \sum_{r=1}^{\ell} J_r \tag{C.2.1}$$

where ℓ = number of modes controlled

J_r = Performance Index Associated with the r^{th} mode, and it is defined by

$$J_r = \frac{1}{2}\int_0^{t_f} (\omega_r^2\xi_r^2 + \dot{\xi}_r^2 + R_r Z_{cr}^2)dt \qquad (C.2.2)$$

$r = 1,2,\ldots,\ell$

t_f = final time

R_r = A parameter to be chosen by the designer. It represents the penalty imposed on the control effort Z_{cr}.

The term $(\omega_r^2\xi_r^2 + \dot{\xi}^2)$ in Eq. (C.2.2) represents the (strain energy + Kinetic Energy) associated with the r^{th} mode.

According to Eq. (C.1.10), Z_{cr} depends only on ξ_r and $\dot{\xi}_r$. Hence, each performance index J_r can be minimized independently of any other modal performance index. For the r^{th} mode, therefore, the optional control problem reduces to the problem of minimizing J_r subject to the constraint conditions (C.1.9).

For the case when $t_f \to \infty$ the control force is given by (see Ref. [77])

$$Z_{cr}(t) = \omega_r(\omega_r - \sqrt{\omega_r^2 + R_r^{-1}}) - [2\omega_r(-\omega_r + \sqrt{\omega_r^2 + R_r^{-1}}) + R^{-1}]^{1/2}\,\dot{\xi}_r(t) \qquad (C.2.3)$$

Substituting Z_{cr} from Eq. (C.2.3) into Eq. (C.2.2) one gets

$$J_r = \frac{\omega_r^2}{2} \int_0^\infty [J_{11}\xi_r^2 + J_{22}\eta_r^2 + J_{12}\xi_r\eta_r]dt \qquad (C.2.4)$$

where $$\eta_r = \frac{\dot{\xi}_r}{\omega_r} \qquad (C.2.5)$$

and

$$J_{11} = 1 + \frac{K_{12}^2}{\omega_r^2 R_r}\ ,\ J_{12} = \frac{2K_{12}K_{22}}{\omega_r^2 R_r}\ ,\ J_{22} = 1 + \frac{K_{22}^2}{\omega_r^2 R_r} \qquad (C.2.6)$$

$$K_{11} = [\frac{1}{\omega_r^2} + \frac{2}{\omega_r R_r}(\omega_r^2 R_r^2 + R_r)^{3/2} - 2R_r^2\omega_r^2 - R_r]^{1/2}$$

$$K_{22} = (R_r - 2\omega_r^2 R_r^2 + 2\omega_r R_r \sqrt{\omega_r^2 R_r^2 + R_r})^{1/2}$$

$$K_{12} = K_{21} = -\omega_r R_r + \sqrt{\omega_r^2 R_r^2 + R_r} \qquad (C.2.7)$$

Solution of the closed loop modal equations for the controlled modes gives

$$\xi_r(t) = e^{-a_1 t}\{\alpha_1 \cos\theta t + \beta_1 \sin\theta t\} \qquad (C.2.8)$$

with $a_1 = \lambda_r\omega_r$

$$\theta = (\omega_d)_r$$

$$\alpha_1 = \xi_r(0)$$

$$\beta_1 = \frac{\omega_r}{(\omega_d)_r}\left(\xi_r(0)\lambda_r + \eta_r(0)\right)$$

$$\alpha_2 = \eta_r(0)$$

$$\beta_2 = \frac{1}{(\omega_d)_r}\left[\xi_r(0)(f_{21}-\omega_r)-\eta_r(0)\omega_r\lambda_r\right]$$

$$\lambda_r = -\frac{f_{22}}{2\omega_r}$$

$$(\omega_d)_r = \left(\omega_r^2 - \omega_r f_{21} - \frac{f22}{4}\right)^{1/2}$$

$$f_{21} = -R_r^{-1}K_{22} \qquad \text{(C.2.9)}$$

Substituting $\xi_r(t)$ from Eq. (C.2.8) into Eq. (C.2.5), (C.2.4) and integrating one obtains

$$J_r = \frac{\omega_r^2}{2}\left(EI_{11} + FI_{22} + GI_{12}\right) \qquad \text{(C.2.10)}$$

with

$$E = J_{11}\alpha_1^2 + J_{22}\alpha_2^2 + J_{12}\alpha_1\alpha_2$$

$$F = J_{11}\beta_1^2 + J_{22}\beta_2^2 + J_{12}\beta_1\beta_2$$

$$G = 2J_{11}\alpha_1\beta_1 + 2J_{22}\alpha_2\beta_2 + J_{12}(\alpha_1\beta_2 + \alpha_2\beta_1)$$

$$I_{11} = \frac{1}{4a_1} + \frac{a_1}{4a_1^2 + \theta^2}$$

$$I_{22} = -\frac{a_1}{4a_1^2 + \theta^2} + \frac{1}{4a_1}$$

$$I_{12} = \frac{1}{4}\left(\frac{\theta}{a_1^2 + \theta^2}\right) \qquad \text{(C.2.11)}$$

Appendix D

DISCRETIZATION AND FINITE ELEMENT MODELING

D.1 Shear Deformable Plate Bending Element

Recent developments in the analysis of orthotropic laminated plates indicate that the thickness effect on the behavior of such plates is more pronounced than in isotropic plates [108]. The classical thin plate theory assumes that normals to the midsurface before deformation remain straight and normal to the midsurface after deformation, implying that transverse shear deformation effects are zero. As a result, the free vibration frequencies, for example, calculated using the thin plate theory are higher than those obtained by the Mindlin plate theory [109].

A number of shear deformable theories for laminates have been proposed to date. The first such theory for laminates isotropic plates is due to Stavsky [110]. The theory has been generalized to laminated anisotropic plates by Yang, Norris and Stavsky [111]. It has been shown by Sun and Whitney [112] and Srinivas and Rao [113] that the Yang-Norris-Stavsky (YNS) theory is adequate for predicting the overall behavior such as transverse deflections and natural frequencies (first few modes) of laminated anisotropic plates. The plate bending element developed here is based on the work by Reddy, Whitney, and Bert [104,114,115].

Laminated Plate Theory of Yang-Norris-Stavsky (YNS)

Consider a plate of constant thickness h composed of a finite-number, n, of thin anisotropic layers oriented at angles

$\theta_1, \theta_2, \ldots, \theta_N$. The origin of the co-ordinate system is located within the middle plane (x-y) with the z-axis being normal to the mid-plane. The material of each layer is assumed to possess a plane of elastic symmetry parallel to the x-y plane.

The YNS theory is based on the following assumed displacement field:

$$\begin{aligned} u &= u_o(x,y,t) + z\,\psi_x(x,y,t) \\ v &= v_o(x,y,t) + z\,\psi_y(x,y,t) \\ w &= w(x,y,t) \end{aligned} \tag{D.1.1}$$

where u, v and w are the displacement components in the x, y and z directions, respectively, u_o and v_o are the in-plane (stretching) displacements of the middle plane, and ψ_x and ψ_y are the shear rotations.

For a symmetric laminate, the equations of motion associated with the YNS theory are

$$\begin{aligned} &\frac{\partial Q_1}{\partial x} + \frac{\partial Q_2}{\partial y} = p\,\frac{\partial^2 w}{\partial t^2} - P \\ &\frac{\partial M_1}{\partial x} + \frac{\partial M_6}{\partial x} - Q_x = I\,\frac{\partial^2 \psi_x}{\partial t^2} \\ &\frac{\partial M_6}{\partial x} + \frac{\partial M_2}{\partial y} - Q_y = I\,\frac{\partial^2 \psi_y}{\partial t^2} \end{aligned} \tag{D.1.2}$$

where

$$(p,\ I) = \int_{-h/2}^{h/2} (1,\ z^2)\ \rho^{(m)}\, dz \tag{D.1.3}$$

$$(Q_x, Q_y) = \int_{-h/2}^{h/2} (\tau_{xz}, \tau_{yz})\, dz \qquad (D.1.4)$$

$$(M_1, M_2, M_6) = \int_{-h/2}^{h/2} (\sigma_x, \sigma_y, \tau_{xy})\, z\, dz$$

$\rho^{(m)}$ being the material density of layer m, and P = P(x,y) is the transversely distributed load. Combining the plate compatibility and constitutive equations one obtains

$$Q_x = A_{44} \left(\frac{\partial w}{\partial x} + \psi_x\right)$$

$$Q_y = A_{55} \left(\frac{\partial w}{\partial y} + \psi_y\right)$$

$$M_1 = D_{11} \frac{\partial \psi_x}{\partial x} + D_{12} \frac{\partial \psi_y}{\partial y} \qquad (D.1.5)$$

$$M_2 = D_{12} \frac{\partial \psi_x}{\partial x} + D_{22} \frac{\partial \psi_y}{\partial y}$$

$$M_6 = D_{66} \left(\frac{\partial \psi_x}{\partial y} + \frac{\partial \psi_y}{\partial x}\right)$$

The material components A_{ij}, D_{ij} are given by

$$(A_{ij}, D_{ij}) = \int_{-h/2}^{h/2} Q_{ij}^{(m)}\, (1, z^2) dz \qquad i,j = 1,2,6 \qquad (D.1.6)$$

$$A_{ij} = k_\alpha k_\beta \bar{A}_{ij}\,, \quad \bar{A}_{ij} = \int_{-k/2}^{k/2} Q_{ij}^{(m)} dz$$

$$(i,j) = 4,5 \quad \alpha = 6 - i \quad , \quad \beta = 6 - j$$

The stiffness coefficients $Q_{ij}^{(m)}$ depend on the material properties and orientation of the m^{th} layer. The parameters k_i are the shear correction factors.

The strain energy and the kinetic energy associated with equations (D.1.2) and (D.1.5) are given by

$$V = V_1 + V_2 \tag{D.1.7}$$

$$T = \frac{1}{2}\int_{\Omega}\{p(\frac{\partial w}{\partial t})^2 + I[(\frac{\partial \psi_x}{\partial t}) + (\frac{\partial \psi_y}{\partial t})^2]\}dxdy \tag{D.1.8}$$

where

$$U_1 = D_{11}(\frac{\partial \psi_x}{\partial x})^2 + 2D_{16}\frac{\partial \psi_x}{\partial x}\frac{\partial \psi_x}{\partial y} + D_{66}(\frac{\partial \psi_x}{\partial y})^2 + \frac{\partial \psi_x}{\partial x}(D_{12}\frac{\partial \psi_y}{\partial y} + 2D_{16}\frac{\partial \psi_y}{\partial x}) + \frac{\partial \psi_y}{\partial y}(D_{12}\frac{\partial \psi_x}{\partial x} + 2D_{26}\frac{\partial \psi_x}{\partial y}) + 2D_{66}\frac{\partial \psi_x}{\partial y}\frac{\partial \psi_y}{\partial y} + D_{66}(\frac{\partial \psi_y}{\partial x})^2\}dxdy \tag{D.1.9}$$

$$U_2 = \frac{1}{2}\int_{\Omega}\{[A_{55}(\frac{\partial w}{\partial x} + \psi_x) + A_{45}(\frac{\partial w}{\partial y} + \psi_y)](\frac{\partial w}{\partial x} + \xi_x) + [A_{45}(\frac{\partial w}{\partial x} + \psi_x) + A_{44}(\frac{\partial w}{\partial y} + \psi_y)](\frac{\partial w}{\partial y} + \psi_y)\}dxdy \tag{D.1.10}$$

D.2 Penalty Formulation of the Equations

The assumption of the classical thin plate theory that the normals to the midsurface before deformation remain straight and normal to the midsurface after deformation implies that

$$\psi_x = -\frac{\partial w}{\partial x} \text{ and } \psi_y = -\frac{\partial w}{\partial y} \tag{D.2.1}$$

If ψ_x and ψ_y from Eq. (D.2.1) are substituted into Eq. (D.1.9), one gets the strain energy $U = U_1$ associated with the classical thin plate

theory. In that case U_1 involves the second-order derivatives of the transverse deflection, and the associated (conventional) finite element formulation results in complicated elements (with many degrees-of-freedom).

To avoid this difficulty, Eq. (D.2.1) is not satisfied explicitly but a penalty method is employed to ensure its approximate satisfaction.

The problem of finding the solution to the thin plate equations can be viewed as one of minimizing the total potential energy $\pi_1 = U_1 + V_1$ where U_1 is the strain energy given by Eq. (D.1.9) in terms of w, and V is the potential of applied loads. Alternatively, the problem can also be viewed as one of finding w,ψ_x,ψ_y subject to the constraint conditions in (D.2.1). The constraints are incorporated by the penalty function method. When the penalty function method is used, the modified functional is given by

$$\pi_p = U_1 + U_p + V \tag{D.2.3}$$

where the penalty function U_p is chosen to be

$$U_p = \frac{1}{2}\int_\Omega [\varepsilon_1^2(\frac{\partial w}{\partial x} + \psi_x)^2 + \varepsilon_2^2(\frac{\partial w}{\partial y} + \psi_y)^2 + 2\varepsilon_1\varepsilon_2(\frac{\partial w}{\partial x} + \psi_x)(\frac{\partial w}{\partial y} + \psi_y)]dxdy \tag{D.2.4}$$

where ε_1 anad ε_2 are the penalty parameters. In the limit as $\varepsilon_1,\varepsilon_2 \to \infty$, the constraints are exactly satisfied.

From the Euler-Lagrange equations of the functional π_p it follows that

$$Q_x = \varepsilon_1^2\left(\frac{\partial w}{\partial x} + \psi_x\right) + \varepsilon_1\varepsilon_2\left(\frac{\partial w}{\partial y} + \psi_y\right)$$

$$Q_y = \varepsilon_1\varepsilon_2\left(\frac{\partial w}{\partial x} + \psi_x\right) + \varepsilon_2^2\left(\frac{\partial w}{\partial y} + \psi_y\right)$$

$$\varepsilon_1^2 = k_1^2\bar{A}_{44},\ \varepsilon_1\varepsilon_2 = k_1k_2\bar{A}_{45},\ \varepsilon_2^2 = k_2^2\bar{A}_{55} \qquad \text{(D.2.5)}$$

This correspondence implies that for very large values of ε_i, the equations govern the thin plate thoery, and for values of ε_i given in (D.2.5) the equations coincide with the YNS theory.

D.3 Plate Bending Finite Element Model

The present finite element model is based on using $\pi_p(w,\psi_x,\psi_y)$ of Eq. (D.2.3) and T of Eq. (D.1.8). For each elemente Ω_e, the same kind of interpolation for all of the variables is assumed

$$w_0^e = \sum_i^n w_i^e N_i^e$$

$$\psi_{x0}^e = \sum_i^n \psi_{xi}^e N_i^e \qquad \text{(D.3.1)}$$

$$\psi_{y0}^e = \sum_i^n \psi_{yi}^e N_i^e$$

where n = nodes per element.

N_i^e are the element interpolation functions, and w_i^e, ψ_{xi}^e, ψ_{yi}^e are the nodal values of w_0^e, ψ_{x0}^e and ψ_{y0}^e, respectively. Substituting (D.3.1) into the first variation of $\pi_p^e(w,\psi_x,\psi_y)$, and collecting the coefficients of the variations δw_i, $\delta\psi_{xi}$, $\delta\psi_{yi}$ one obtains

$$[M^e]\{\ddot{\Delta}^e\} + [K^e]\{\Delta^e\} = \{F^e\} \qquad \text{(D.3.2)}$$

where

$$\{\Delta^e\} = \begin{Bmatrix} \{w^e\} \\ \{\psi_x^e\} \\ \{\psi_y^e\} \end{Bmatrix} \tag{D.3.3}$$

$$[M] = \begin{bmatrix} p[S^{oo}] & & \\ & I[S^{oo}] & \\ & & I[S^{oo}] \end{bmatrix} \tag{D.3.4}$$

$$[K] = \begin{bmatrix} [K^{11}] & [K^{12}] & [K^{13}] \\ [K^{12}]^T & [K^{22}] & [K^{23}] \\ [K^{13}]^T & [K^{23}]^T & [K^{33}] \end{bmatrix} \tag{D.3.5}$$

and

$$K_{ij}^{11} = \int_{\Omega e} \left(A_{55} \frac{\partial \psi_i}{\partial x} \frac{\partial \psi_j}{2x} + A_{44} \frac{\partial \psi_i}{\partial y} \frac{\partial \psi_j}{\partial y}\right) dxdy$$

$$K_{ij}^{12} = \int_{\Omega e} A_{55} \frac{\partial \psi_i}{\partial x} \psi_j \, dxdy$$

$$K_{ij}^{13} = \int_{\Omega e} A_{44} \frac{\partial \psi_i}{\partial y} \psi_j \, dxdy$$

$$K_{ij}^{22} = \int_{\Omega e} \left(D_{11} \frac{\partial \psi_i}{\partial x} \frac{\partial \psi_j}{\partial x} + D_{66} \frac{\partial \psi_i}{\partial y} \frac{\partial \psi_j}{\partial y} + A_{55} \psi_i \psi_j\right) dxdy$$

$$K_{ij}^{23} = \int_{\Omega e} \left(D_{12} \frac{\partial \psi_i}{\partial x} \frac{\partial \psi_j}{\partial y} + D_{66} \frac{\partial \psi_i}{\partial y} \frac{\partial \psi_j}{\partial y}\right) dxdy$$

$$K^{33}_{ij} = \int_{\Omega e} \left(D_{66} \frac{\partial \psi_i}{\partial x} \frac{\partial \psi_j}{\partial x} + D_{22} \frac{\partial \psi_i}{\partial y} \frac{\partial \psi_j}{\partial y} + A_{44}\, \psi_i \psi_j\right) dxdy$$

$$S^{00}_{ij} = \int_{\Omega e} \psi_i \psi_j \, dxdy \qquad \text{(D.3.6)}$$

D. 4 Constitutive Equations for Orthotropic Plies

For an orthotropic material, the compliance matrix components in terms of the engineering constants are

$$[S] = \begin{bmatrix} \frac{1}{E_1} & -\frac{\nu_{21}}{E_2} & -\frac{\nu_{31}}{E_3} & 0 & 0 & 0 \\ -\frac{\nu_{12}}{E_1} & \frac{1}{E_2} & -\frac{\nu_{32}}{E_3} & 0 & 0 & 0 \\ -\frac{\nu_{13}}{E_1} & -\frac{\nu_{23}}{E_2} & \frac{1}{E_3} & 0 & 0 & 0 \\ 0 & 0 & 0 & \frac{1}{G_{23}} & 0 & 0 \\ 0 & 0 & 0 & 0 & \frac{1}{G_{31}} & 0 \\ 0 & 0 & 0 & 0 & 0 & \frac{1}{G_{12}} \end{bmatrix} \qquad \text{(D.4.1)}$$

E_1, E_2, E_3 are the Young's moduli in 1,2, and 3 directions, respectively:

ν_{ij} = the Poisson's ratio for transverse strain in the j-direction when stressed in the i-th direction and G_{23},G_{31},G_{12} are the shear moduli in the 2-3, 3-1 and 1-2 planes, respectively.

The stresses and strains in the principal co-ordinate system are related by the relation

$$\{\varepsilon\} = [S]\{\sigma\} \tag{D.4.2}$$

where

$$\{\varepsilon\}^T = (\varepsilon_1, \varepsilon_2, \varepsilon_3, \gamma_{23}, \gamma_{13}, \gamma_{12}) \tag{D.4.3}$$

$$\{\sigma\}^T = (\sigma_1, \sigma_2, \sigma_3, \tau_{23}, \tau_{13}, \tau_{12}) \tag{D.4.4}$$

In this work, normal stress $\sigma_3 = 0$. The principal stress strain relations reduce to

$$\begin{Bmatrix} \varepsilon_1 \\ \varepsilon_2 \\ \gamma_{12} \end{Bmatrix} = \begin{bmatrix} S_{11} & S_{12} & 0 \\ S_{12} & S_{22} & 0 \\ 0 & 0 & S_{66} \end{bmatrix} \begin{Bmatrix} \sigma_1 \\ \sigma_2 \\ \tau_{12} \end{Bmatrix} \tag{D.4.5}$$

$$\begin{Bmatrix} \gamma_{23} \\ \gamma_{13} \end{Bmatrix} = \begin{bmatrix} S_{44} & 0 \\ 0 & S_{55} \end{bmatrix} \begin{Bmatrix} \tau_{23} \\ \tau_{13} \end{Bmatrix} \tag{D.4.6}$$

The inverse relation can be written as

$$\begin{Bmatrix} \sigma_1 \\ \sigma_2 \\ \tau_{12} \end{Bmatrix} = \begin{bmatrix} Q_{11} & Q_{12} & 0 \\ Q_{12} & Q_{22} & 0 \\ 0 & 0 & Q_{66} \end{bmatrix} \begin{Bmatrix} \varepsilon_1 \\ \varepsilon_2 \\ \gamma_{12} \end{Bmatrix} \tag{D.4.7}$$

$$\begin{Bmatrix} \tau_{23} \\ \tau_{13} \end{Bmatrix} = \begin{bmatrix} Q_{44} & 0 \\ 0 & Q_{55} \end{bmatrix} \begin{Bmatrix} \gamma_{23} \\ \gamma_{13} \end{Bmatrix} \tag{D.4.8}$$

where

$$Q_{11} = \frac{S_{22}}{S_{11}S_{22} - S_{12}^2}$$

$$Q_{12} = -\frac{S_{11}}{S_{11}S_{22} - S_{12}^2} \qquad \text{(D.4.9)}$$

$$Q_{22} = \frac{S_{11}}{S_{11}S_{22} - S_{12}^2}$$

$$Q_{66} = \frac{1}{S_{66}}$$

The stresses in the two co-ordinate systems are related by

$$\begin{Bmatrix} \sigma_1 \\ \sigma_2 \\ \tau_{12} \end{Bmatrix} = [T] \begin{Bmatrix} \sigma_x \\ \sigma_y \\ \tau_{xy} \end{Bmatrix} \qquad \text{(D.4.10)}$$

$$\begin{Bmatrix} \tau_{23} \\ \tau_{13} \end{Bmatrix} = \begin{bmatrix} m & -n \\ n & m \end{bmatrix} \begin{Bmatrix} \tau_{yz} \\ \tau_{xy} \end{Bmatrix} \qquad \text{(D.4.11)}$$

where

$$[T] = \begin{bmatrix} m^2 & n^2 & 2mn \\ n^2 & m^2 & -2mn \\ -mn & mn & m^2 - n^2 \end{bmatrix} \qquad \text{(D.4.12)}$$

with $m = \cos\theta$, $n = \sin\theta$, θ being the angle between the principal material directions and the x-y co-ordinate system.

After algebraic manipulation, the constitutive equations in the x-y co-ordinate system are

$$\begin{Bmatrix}\sigma_x\\ \sigma_y\\ \tau_{xy}\end{Bmatrix} = \begin{bmatrix}Q_{11} & Q_{12} & Q_{16}\\ Q_{12} & Q_{22} & Q_{26}\\ Q_{16} & Q_{26} & Q_{66}\end{bmatrix}\begin{Bmatrix}\varepsilon_x\\ \varepsilon_y\\ \gamma_{xy}\end{Bmatrix} \qquad (D.4.13)$$

$$\begin{Bmatrix}\tau_{yz}\\ \tau_{xz}\end{Bmatrix} = \begin{bmatrix}Q_{44} & Q_{45}\\ Q_{45} & Q_{55}\end{bmatrix}\begin{Bmatrix}\gamma_{yz}\\ \gamma_{xz}\end{Bmatrix} \qquad (D.4.14)$$

where

$$\begin{bmatrix}\bar{Q}_{11} & \bar{Q}_{12} & \bar{Q}_{16}\\ \bar{Q}_{12} & \bar{Q}_{22} & \bar{Q}_{26}\\ \bar{Q}_{16} & \bar{Q}_{26} & \bar{Q}_{66}\end{bmatrix} = [T]^{-1}\begin{bmatrix}Q_{11} & Q_{12} & 0\\ Q_{12} & Q_{22} & 0\\ 0 & 0 & Q_{66}\end{bmatrix}[T]^{-T} \qquad (D.4.15)$$

and

$$\begin{bmatrix}\bar{Q}_{44} & \bar{Q}_{45}\\ \bar{Q}_{45} & \bar{Q}_{55}\end{bmatrix} = \begin{bmatrix}m & n\\ -n & m\end{bmatrix}\begin{bmatrix}G_{23} & 0\\ 0 & G_{13}\end{bmatrix}\begin{bmatrix}m & -n\\ n & m\end{bmatrix} \qquad (D.4.16)$$

D.5 Isoparametric Elements and Numerical Integration

The plate is modelled using 8-noded isoparametric plate bending elements. Fig. 3 shows one such typical element. For each element, the displacements are interpolated using the relations

$$w = \sum_{i}^{n} w_i N_i$$

$$\psi_y = \sum_i^n \psi_{yi} N_i$$

$$x = x(\xi, \eta) = \sum_{i=1}^{n} x_i N_i$$

$$y = y(\xi,\eta) = \sum_{i=1}^{n} y_i N_i \qquad (D.5.1)$$

where n is the number of nodes per element, N_i are the element interpolation functions and w_i, ψ_{xi}, ψ_{yi} are nodal values of w, ψ_x, ψ_y respectively, x_i, y_i are the x and y co-ordinates, respectively, of the element nodes. It should be noted that the same functions that are used to interpolate displacements are also used to transform each element in the mesh to a master element. The master element is bounded by the lines $\xi = \pm 1$ and $\eta = \pm 1$, as shown in Fig. 3.

The reason for the transformation is the ease with which integrations can be performed over the master element, which has a square shape. The original element could be non-rectangular and curved sided in general, and as such presents formidable problems for integrations, necessary to compute the elements of the mass and stiffness matrices. Numerical integration using Gauss quadrature is used for this purpose. For the master element shown in Fig. 3, the interpolation funcions can be shown to be

$$N_i(\xi,\eta) = \frac{1}{4}(1 + \xi\xi_i)(1 + \eta\eta_i)(\xi\xi_i + \eta\eta_i - 1) \quad i = 1,2,3,4$$

$$N_i(\xi,\eta) = \frac{1}{2}(1 - \xi^2)(1 + \eta\eta_i) , \quad i = 5,7$$

$$N_i(\varepsilon,\eta) = \frac{1}{2}(1 - \eta^2)(1 + \xi\xi_i) \quad i = 6,8 \tag{D.5.2}$$

where (ξ_i, η_i) are the intrinsic co-ordinates of the i^{th} mode.

Suppose it is required to evaluate the term

$$K_{ij} = \int_{\Omega e} \left(\frac{\partial N_i}{\partial x}\frac{\partial N_j}{\partial x} + \frac{\partial N_i}{\partial y}\frac{\partial N_j}{\partial y}\right) dxdy \tag{D.5.3}$$

It can be shown [104] that this term can be transformed to

$$K_{ij} = \int_{-1}^{1}\int_{-1}^{1} \left(\frac{\partial N_i}{\partial x}\frac{\partial N_j}{\partial x} + \frac{\partial N_i}{\partial y}\frac{\partial N_j}{\partial y}\right) \det J d\xi d\eta \tag{D.5.4}$$

where $\frac{\partial N_i}{\partial x}$ and $\frac{\partial N_i}{\partial y}$ are given by

$$\begin{Bmatrix} \frac{\partial N_i}{\partial x} \\ \frac{\partial N_i}{\partial y} \end{Bmatrix} = \begin{bmatrix} \frac{\partial \xi}{\partial x} & \frac{\partial \eta}{\partial x} \\ \frac{\partial \xi}{\partial y} & \frac{\partial \eta}{\partial y} \end{bmatrix} \begin{Bmatrix} \frac{\partial N_i}{\partial \xi} \\ \frac{\partial N_i}{\partial \eta} \end{Bmatrix} = [J]^{-1} \begin{Bmatrix} \frac{\partial N_i}{\partial \xi} \\ \frac{\partial N_i}{\partial \eta} \end{Bmatrix} \tag{D.5.5}$$

[J] being the Jacobian of transformation.

The integrand in Eq. (D.5.4) is thus a function of the intrinsic coordinates ξ and η. Thus, numerical integration based on Gauss-Legender quadrature yields

$$K_{ij} = \int_{-1}^{1}\int_{-1}^{1} F(\xi,\eta)\, d\xi d\eta \tag{D.5.6}$$

$$= \sum_{I=1}^{N}\sum_{J=1}^{N} F(Z_I, Z_J) W_I W_J \tag{D.5.7}$$

where N is the number of Gaussian points, Z_I re the intrinsic co-ordinates of the Gauss points, and W_I are the corresponding weights.

D.7 Frame Element

The stiffners are modelled using frame elements. A space frame element is a straight bar of uniform cross section which is capable of resisting axial forces, bending moments about two principal axes in the plane of its cross section and twisting moment about its centroidal axis. The corresponding degrees of freedom are shown in Fig. 5. The axial displacements q_1 and q_7 depend only on the axial forces, and the torsional displacements q_4 and q_{10} depend only on the torsional moments. If the xy and xz planes coincide with the principal planes of the cross section, the bending displacements and forces in the two planes can be considered to be independent of each other.

Thus the displacements can be separated into four groups (axial, torsional, bending in the xy palne, bending in the xz plane) each of which can be considered independently of the others. Let $u(x)$, $\theta(x)$ be the axial, torsional displacements and $v(x)$, $w(x)$ be the displacements due to bending in the xy and xz plane respectively. The assumed displacements are of the form

$$u(x) = \alpha_1 + \alpha_2 x \tag{D.7.1}$$

$$\theta(x) = \alpha_3 + \alpha_4 x \tag{D.7.2}$$

$$v(x) = \alpha_5 + \alpha_6 x + \alpha_7 x^2 + \alpha_8 x^3 \tag{D.7.3}$$

$$w(x) = \alpha_9 + \alpha_{10} x + \alpha_{11} x^2 + \alpha_{12} x^3 \tag{D.7.4}$$

Let L,A,J denote the length, the cross-sectional area and the polar moment of inertia of the frame element. Also let I_{yy} and I_{zz} denote the area moment of Inertia about the z and y axis and E and G denote the Young's modulus and shear modulus respectively. Then, the stiffness and mass matrices corresponding to the assumed displacements in (D.7.1) - (D.7.4) can be derived to be

$$\text{Axial Stiffness Matrix } [K_a^{(e)}]_{2\times 2} = \frac{AE}{L} \begin{matrix} \\ q_1 \\ q_2 \end{matrix} \overset{\begin{matrix} q_1 & q_2 \end{matrix}}{\begin{bmatrix} 1 & -1 \\ -1 & 1 \end{bmatrix}} \tag{D.7.5}$$

$$\text{Axial Mass Matrix } [M_a^{(e)}]_{2\times 2} = \rho AL \begin{matrix} \\ q_1 \\ q_2 \end{matrix} \overset{\begin{matrix} q_1 & q_2 \end{matrix}}{\begin{bmatrix} \frac{1}{3} & \frac{1}{6} \\ \frac{1}{6} & \frac{1}{3} \end{bmatrix}} \tag{D.7.6}$$

$$\text{Torsional Stiffness Matrix } [K_t^{(e)}]_{2\times 2} = \frac{GJ}{L} \begin{matrix} \\ q_4 \\ q_{10} \end{matrix} \overset{\begin{matrix} q_4 & q_{10} \end{matrix}}{\begin{bmatrix} 1 & -1 \\ -1 & 1 \end{bmatrix}} \tag{D.7.7}$$

$$\text{Torsional Mass Matrix } [M_{(t)}^{(e)}]_{2\times 2} = \rho JL \begin{matrix} \\ q_4 \\ q_{10} \end{matrix} \overset{\begin{matrix} q_4 & q_{10} \end{matrix}}{\begin{bmatrix} \frac{1}{3} & \frac{1}{6} \\ \frac{1}{6} & \frac{1}{3} \end{bmatrix}} \tag{D.7.8}$$

Stiffness matrix for bending in the xy plane

$$[K_{xy}^{(e)}] = \frac{EI_{zz}}{L^3} \begin{matrix} \\ q_2 \\ q_6 \\ q_8 \\ q_{12} \end{matrix} \begin{matrix} \begin{matrix} q_2 & q_6 & q_8 & q_{12} \end{matrix} \\ \begin{bmatrix} 12 & 6L & -12 & 6L \\ 6L & 4L^2 & -6L & 2L^2 \\ -12 & -6L & 12 & -6L \\ 6L & 2L^2 & -6L & 4L^2 \end{bmatrix} \end{matrix} \qquad (D.7.9)$$

Mass matrix for bending in the x - y plane

$$[M_{xy}^{(e)}] = \rho AL \begin{matrix} \\ q_2 \\ q_6 \\ q_8 \\ q_{12} \end{matrix} \begin{matrix} \begin{matrix} q_2 & q_6 & q_8 & q_{12} \end{matrix} \\ \begin{bmatrix} \frac{13}{35} & \frac{11}{210}L & \frac{9}{70} & -\frac{13}{420}L \\ \frac{11}{210}L & \frac{L^2}{105} & \frac{13}{420}L & -\frac{L^2}{140} \\ \frac{9}{70} & \frac{13}{420}L & \frac{13}{35} & -\frac{11}{210}L \\ -\frac{13}{420}L & -\frac{L^2}{140} & -\frac{11}{210}L & \frac{L^2}{105} \end{bmatrix} \end{matrix} \qquad (D.7.10)$$

Stiffness matrix for bending in the x - z plane

$$[K_{xz}^{(e)}] = \frac{EI_{yy}}{L^3} \begin{matrix} \\ q_3 \\ q_5 \\ q_9 \\ q_{11} \end{matrix} \begin{matrix} \begin{matrix} q_3 & q_5 & q_9 & q_{11} \end{matrix} \\ \begin{bmatrix} 12 & 6L & -12 & 6L \\ 6L & 4L^2 & -6L & 2L^2 \\ -12 & -6L & 12 & -6L \\ 6L & 2L^2 & -6L & 4L^2 \end{bmatrix} \end{matrix} \qquad (D.7.11)$$

Mass matrix for bending in the x - z plane

$$
[M_{xz}^{(e)}] = \rho AL
\begin{array}{c}
\begin{matrix} q_3 & q_5 & q_9 & q_{11} \end{matrix} \\
\begin{bmatrix}
\frac{13}{35} & -\frac{11}{210}L & \frac{9}{70} & \frac{13L}{420} \\
-\frac{11}{210}L & \frac{L^2}{105} & -\frac{13}{420}L & -\frac{L^2}{140} \\
\frac{9}{70} & -\frac{13}{420}L & \frac{13}{35} & \frac{11}{210}L \\
\frac{13L}{420} & -\frac{L^2}{140} & \frac{11}{210}L & \frac{L^2}{105}
\end{bmatrix}
\begin{matrix} q_3 \\ q_5 \\ q_9 \\ q_{11} \end{matrix}
\end{array}
\qquad (D.7.12)
$$

The complete element stiffness matrix with $q_1, q_2 \ldots q_{12}$ degrees of freedom is assembled from the submatrices given by relations (D.7.5), (D.7.7), (D.7.9) and (D.7.11). Similarly the element mass matrix is assembled from the submatrices given in relations (D.7.6), (D.7.8), (D.7.10), (D.7.12).

Appendix E

E.1 Calculation of Eigenvalue S

Structural Frequencies are claculated by solving the generalized Eigenvalue Problem

$$Kx = \lambda Mx \qquad (E.1.1)$$

where K and M are, respectively, the stiffness matrix and mass matrix of the finite element assemblage. The eigenvalues λ_i and the eigenvectors x_i are the free vibration frequencies (rad/sec) squared, ω_i^2, and corresponding modeshapes respectively.

E.2. Skyline Storage for K and M matrices:

To exploit the symmetry and sparsity of the K and M matrices, skyline storage scheme is employed. For symmetric matrix, only the upper (or lower) triangular part of the matrix need be stored. For the matrices K, M the skyline (column heights, h_i, $i = 1,2,\ldots,n$) is determined by the connectivity of the finite element assemblage. For consistent K, M matrices, corresponding skylines are identical.

The skyline storage scheme is efficient in terms of memory requirements (by not storing the zero elements) and also requires less computations during matrix operations by eliminating operations on elements that have values equal to zero.

E.3 Matrix Decomposition:

Often it is necessary to solve the set of equations, for the unknown x

$$Kx = R \tag{E.3.1}$$

where K is the stiffness matrix and R is a given vector.

In static analysis x is the vector of unknown displacements while R is the known vector of applied loads. The reason for discussing the solution of Eq. (E.3.1), here, is that it occurs quite frequently during the solution of eigenvalue problems.

As K is symmetric, it can be decomposed into upper and lower triangular matrices, using Cholesky method.

$$K = LDL^T \tag{E.3.2}$$

where L = Lower Triangular matrix with all diagonal elements equal to unity

L^T = Transpose of L

D = Diagonal Matrix

Solution of Eq. (E.3.1) is performed using forward and backward substitution as follows.

Solve for the unknown Z using forward substitution in the equation

$$(LD)Z = R \tag{E.3.3}$$

Backward substitution is then used to solve for x, using the relation

$$L^T x = Z \tag{E.3.4}$$

In computer implementation only L and D need to be stored. An important property of the decomposition shown in Eq. (E.3.2) is that L^T has the same skyline as the matrix K. Thus the sparsity of K is preserved. Also as all the diagonal elements of L^T are equal to unity, these need not be stored, instead, the elements of D in Eq. (E.3.2) can be stored in corresponding locations.

The solution of Eq. (E.3.1) can thus be carried out conveniently using Cholesky decomposition and the skyline storage scheme discussed in Section E.2. Computationally this is an efficient method as it minimizes memory requirements and also the computation time by elimination of operations with matrix elements that have a value equal to zero.

E.4 Inverse Iteration

The technique of inverse iteration is very effectively used to calculate an eigenvector, and at the same time the corresponding eigenvalue while exploring the sparsity and symmetry of the K and M matrices.

In the following the basic equations used in inverse iteration are presented. Let λ_1, x_1 be the lowest eigenvalue and corresponding eigenvector satisfying the generalized eigenvalue problem of Eq. (E.1.1). Let $y_1, y_2, y_3, \ldots y_\ell$ be the eigenvector approximations obtained after the 1st,2nd,3rd,...ℓth iteration. Then as $\ell \to \infty$, $y_\ell \to x_1$.

Starting with an eigenvector y_1, evaluate for $\ell = 1,2,\ldots$

$$K\bar{y}_{\ell+1} = My_\ell = z_\ell \tag{E.4.1}$$

$$\bar{z}_{\ell+1} = M\bar{y}_{\ell+1} \tag{E.4.2}$$

$$\rho = \frac{\bar{y}_{\ell+1}^T \bar{z}_\ell}{\bar{y}_{\ell+1}^T \bar{z}_{\ell+1}} \tag{E.4.3}$$

$$z_{\ell+1} = \frac{\bar{z}_{\ell+1}}{(\bar{y}_{\ell+1}^T \bar{z}_{\ell+1})^{1/2}} \tag{E.4.4}$$

where, provided that $y_1^T x_1 \neq 0$, $y_{\ell+1} \to Mx_1$ and $\rho \to \lambda_1$, as $\ell \to \infty$.

If the scaling in (E.4.4) is not included in the iteration, the elements of the iteration vectors grow (or decrease) in each step and the iteration vectors do not converge to x_1 but to a multiple of it.

The above scaling (Eq. (E.4.4) ensures that the iteration vector tends to a fixed length, such that $\|y_{\ell+1}\| = \|Mx_1\|$ as $\ell \to \infty$

A computationally cheaper scaling is to normalize a given element of the eigenvector to have a value of unity. One can choose any element i for this purpose, provided, that

$$x_1(i) \neq 0 \tag{E.4.5}$$

where x_1 is the required eigenvector. Numerical considerations indicate that i should be chosen such that $x_1(i)$ is the largest (absolute) element of x_1. At the beginning of the iteration process, however, x_1 is not known, so it is not possible to know the largest element of x_1. Instead, i is chosen such that $y_2(i)$ is the largest element of y_2. (y_2 is the vector obtained at the end of the 1st iteration). Chosing i in this fashion has been found to be quite efficient in practice.

The method can be summarized as follows.

Starting with an eigenvector y_1, evaluate for $\ell = 1,2,...$

$$K\bar{y}_{\ell+1} = My_{\ell} \quad . \tag{E.4.6}$$

$$\rho_{\ell+1} = \bar{y}_{\ell+1}(i) \tag{E.4.7}$$

$$y_{\ell+1} = \frac{\bar{y}_{\ell+1}}{\rho_{\ell+1}} \tag{E.4.8}$$

Provided that $y_1^T x_1 \neq 0$,

$$y_{\ell+1} \to \alpha x_1 \tag{E.4.9}$$

$$\rho_{\ell+1} \to \lambda_1 \tag{E.4.10}$$

as $\ell \to \infty$

$$\text{where } \alpha = y_{\ell+1}^T My_{\ell+1} \tag{E.4.11}$$

i is chosen such that $y_2(i)$ = Largest (absolute) element of y_2.

Steps (E.4.7), (E.4.8) need less computations than corresponding steps (E.4.3, (E.4.4). The set of equations given by Eq. (E.4.1) or Eq. (E.4.6) are solved quite efficiently using the method described in section E.3, where symmetry and sparsity are fully exploited. The method described by relations (E.4.1 - E.4.4) is safer to use, when a good starting iteration vector is not available. When a good starting iteration vector is available, it is cheaper to use the method described by the relations (E.4.6 - E.4.11).

E.5 Shifting

An important procedure that is extensively used in the solution of eigenvalues and eigenvectors is shifting. The purpose of shifting is to accelerate the calculations of the required eigenvalues.

Consider the generalized eigenvalue problem

$$\hat{K}Y = \mu MY \tag{E.5.1}$$

where

$$\hat{K} = K - \beta M \tag{E.5.2}$$

K,M are the stiffness and mass matrices respectively.

The eigenvalues and eigenvectors of the eigenvalue problem in (E.5.1) can be shown to be

$$\mu = \lambda - \beta \tag{E.5.3}$$

$$Y = x \tag{E.5.4}$$

where λ, x are the eigenvalues and eigenvectors of the eigenvalue problem

$$Kx = \lambda Mx \tag{E.5.5}$$

It can be shown [116] that by using shifting in conjunction with inverse iteration one can choose a shift near enough to the specific eigenvalue of interest to make the inverse iteration converge to the required eigenpair instead of the first eigenpair.

E.6 Generalized Jacobi Method:

In conjunction with the inverse iteration method discussed in E.3. this method is useful to compute the first few eigenpairs of large order systems. Specifically, it computes all the eigenvalues and eigenvectors of small order systems quite efficiently. The basic property employed by this method is

$$x^T K x = \Lambda \qquad \text{(E.6.1)}$$

$$x^T M x = I \qquad \text{(E.6.2)}$$

The basic scheme is to reduce K and M into diagonal form using successive pre-and post multiplication by matrices P_ℓ^T and P_ℓ respectively, where $\ell = 1,2,\ldots$. where the matrices P_ℓ are selected to bring K and M closer to diagonal form. (See Ref. ?)

E.7. Subspace Iteration:

The Jacobi Transformation method discussed in section E.6 computes all the eigenvalues and eigenvectors of the system $Kx = \lambda Mx$. For Large order systems, however, this method is prohibitively expensive. In this work, only the first few eigenvalues and eigenvectors are of interest, so in the interest of computational efficiency, one needs to use a method capable of computing the first few eigenpairs cheaply.

The inverse iteration method presented in section E.4 can be effectively used for large order systems, however, it computes only the first or lowest eigenvalue and corresponding eigenvector. The basic inverse iteration technique converges to λ_1 and x_1, but this method can be

employed with shifting to calculate other eigenvalues and corresponding eigenvectors. (See Section E.5).

Assume that a specific eigenpair, say (λ_ℓ, x_ℓ) has been calculated using inverse iteration and another pair needs to be computed. To ensure that one does not converge again to (λ_ℓ, x_ℓ), it is required to deflate either the matrices or the iteration vectors.

Matrix deflation, however, destroys the sparsity of the mass and stiffness matrices M and K. For large order systems this is a disadvantage. Secondly, the eigenvectors have to be computed to a very high precision to avoid the accumulation of errors introduced in the deflation process.

Instead of matrix deflation, one can deflate the iteration vector in order to converge to an eigenpair other than (λ_ℓ, x_ℓ). If the iteration vector is orthogonalized to the eigenvectors already calculated, the possibility that the iteration converges to any one of them is eliminated, instead, convergence occurs to another eigenvector.

A particular vector orthogonalization procedure that is employed extensively is the Gram-Schmidt method [116]. However, the Gram-Schmidt method requires that each eigenpair be calculated to a high degree of precsion, and also, the iteration vector needs to be orthogonalized in each iteration.

The subspace iteration method avoids the difficulties encountered with the matrix deflation technique and the Gram-Schmidt method.

The basic objective in the subspace iteration method is to solve for the lowest p eigenvalues and corresponding eigenvectors satisfying

$$Kx = Mx\Lambda \tag{E.7.1}$$

where $\Lambda = \text{diag}(\lambda_i)$ and $x = [x_1, x_2, \ldots, x_p]$

In addition to the relation (E.7.1), the eigenvectors also satisfy the orthogonality conditions

$$x^T K x = \Lambda \; ; \quad x^T M x = I \tag{E.7.2}$$

where I is a unit matrix of order p because x stores only p eigenvectors.

The essential idea of the subspace iteration method uses the fact that the eigenvectors in (E.7.1) form an M-orthonormal basis of the p-dimensional least-dominant subspace of the operators K and M, which is denoted here as E_∞. In the solution the iteration with p linearly independent vectors can therefore be regarded as an iteration with a subspace. The starting iteration vectors span E_1 and iteration continues until, to sufficient accuracy, E_∞ is spanned. The fact that iteration is performed with a subjspace has some consequences. The total number of required iterations depends on how "close" E_1 is to E_∞, and not on how close each iteration vector is to an eigenvector. It is much easier to establish a p-dimensional starting subspace which is close to E_∞ than to find p vectors that each are close to the required eigenvectors. Also, because iteration is performed with a subspace, convergence of the subspace is all that is required and not of individual iteration vectors to eigenvectors. In other words, if the itera-

tion vectors are linear combinations of the required eigenvectors, the solution algorithm converges in a single step.

Consider the simultaneous vector inverse iteration on p vectors. Let x_1 store the p starting iteration vectors, which span the starting subspace E_1. Simultaneous inverse iteration on the p vectors can be written

$$KY_{\ell+1} = MY_{\ell} \tag{E.7.3}$$

It is necessary to keep the p eigenvectors comprising Y_{ℓ}, mutually orthogonal, otherwise all the eigenvectors will converge to the first eigenvector x_1. To achieve this, the following procedure is adopted.

For $\ell = 1,2,\ldots,$ iterate from E_{ℓ} to $E_{\ell+1}$

$$K\bar{Y}_{\ell+1} = MY_{\ell} \tag{E.7.4}$$

Find the projections of the operators K and M onto $E_{\ell+1}$

$$K_{\ell+1} = \bar{Y}^T_{\ell+1} K\bar{Y}_{\ell+1} \tag{E.7.5}$$

$$M_{\ell+1} + Y^T_{\ell+1} M\bar{Y}_{\ell+1} \tag{E.7.6}$$

Solve for the eigensystem of the projected operatoars

$$K_{\ell+1}Q_{\ell+1} = M_{\ell+1}Q_{\ell+1}\Lambda_{\ell+1} \tag{E.7.7}$$

Find an improved approximation to the eigenvectors:

$$Y_{\ell+1} = \bar{Y}_{\ell+1}Q_{\ell+1} \tag{E.7.8}$$

Then, provided that the vectors in Y_1 are not orthogonal to one of the required eigenvectors, $\Lambda_{\ell+1} \to \Lambda$ and $Y_{\ell+1} \to X$ as $k \to \infty$

In the subspace iteration, it is implied that the iteration vectors are ordered in an appropriate way i.e. the iteration vectors converging to $x_1, x_2, \ldots$ are stored as the first, second,... collumns of Y_{k+1}.

The eigenproblem in (E.7.7) can be solved quite efficiently using the Jacobi method described in section E.7. This is so because the eigenproblem in E.7.7 is of order p, which is small.

The set of equations in Eq. E.7.4 is solved by the Cholesky Decomposition of the stiffness matrix K followed by a forward and backward substitution. (See section E.3). The symmetry and sparsity of the mass and stiffness matrices is thus exploited in the solution.

E.8 Starting Iteration Vectors

The first step in the subspace iteration method is the selection of the starting iteration vectors Y_1. If starting vectors that span the least dominant subspace are used, the subspace iteration will converge in one step.

The following choice of starting iteration vectors has been found by experience to be effective. The first eigenvector is simply the diagonal of the mass matrix M, to ensure that all mass degrees of freedom are excited. The other eigenvectors are unit vectors with entries of +1 at the coordinates with the smallest ratios k_{ii}/m_{ii}.

TABLE 1

Nodal Co-ordinates and Boundary Condition Codes for the FEM Mesh.

Node Number	Boundary Condition Code = 0 Free = 1 Fixed			Nodal Coordinate	
	W	ψ_x	ψ_y	x	y
1	1	1	1	0	0.0
2	1	1	0	5.0	0.0
9	1	1	1	40.0	0.0
10	1	0	1	0.0	5.0
11	0	0	0	10.0	5.0
14	1	0	1	40.0	5.0
15	1	0	1	0.0	10.0
16	0	0	0	5.0	10.0
23	1	0	1	40.0	10.0
24	1	0	1	0.0	15.0
25	0	0	0	10.0	15.0
28	1	0	1	40.0	15.0
29	1	0	1	0.0	20.0
30	0	0	0	5.0	20.0
37	1	0	1	40.0	20.0
38	1	0	1	0.0	25.0
39	0	0	0	10.0	25.0
42	1	0	1	40.0	25.0
43	1	0	1	0.0	30.0
44	0	0	0	5.0	30.0
51	1	0	1	40.0	30.0
52	1	0	1	0.0	35.0
53	0	0	0	10.0	35.0
56	1	0	1	40.0	35.0
57	1	1	1	0.0	40.0
58	1	1	0	5.0	40.0
65	1	1	1	40.0	40.0

TABLE 2

Material Properties for Laminate and Stiffeners

Material used: Graphite Epoxy

$$\frac{E_1}{E_2} = 40 \quad , \quad \frac{G_{12}}{E_2} = 0.6 \quad , \quad \frac{G_{23}}{E_2} = 0.5 \quad , \quad \frac{G_{31}}{E_2} = 0.6$$

$$\nu_{12} = \nu_{13} = 0.25$$

$$k_1^2 = k_2^2 = 5/6$$

$\rho = 0.001$ (Mass per unit volume)

TABLE 3

Details of the Initial Design and its Frequencies

i	Integer Variables n_i	Continuous Variables A_i	Structural Eigenvalues $\frac{\lambda_{oi}}{\lambda_{o1}}$
1	2	0.5	1.0
2	2	0.5	3.57
3	2	0.5	9.97
4	2	0.5	10.38
5	2	0.5	16.60
6	1	0.5	22.03
7	1	0.5	32.48
8		0.5	43.61

TABLE 4

Definition of Different Structural Optimization Schemes

Case Number	Case Name	Definition of Objective Function	Frequency Constraints	Parameter Definition
1.a	OPT1a	Maximize λ_1	$\frac{\lambda_{i+1}}{\lambda_i} > r_i$	
1.b	OPT1b	Maximize λ_1	$\frac{\lambda_i}{\lambda_{01}} > r_i$	
2.a	OPT2a	Minimize $\Sigma(\lambda_i-\beta_i)^2$	$\frac{\lambda_i}{\lambda_{01}} > r_i$	$\beta_i=\lambda_{0_{i+1}}$
2.b	OPT2b	Minimize $\Sigma(\lambda_i-\beta_i)^2$	$\frac{\lambda_i}{\lambda_{01}} > r_i$	$\beta_i=1.1\lambda_{0i+1}$
2.c	OPT2c	Minimize $\Sigma(\lambda_i-\beta_i)^2$	$\frac{\lambda_i}{\lambda_{01}} > r_i$	$\beta_i=1.2\lambda_{0_{i+1}}$
2.d	OPT2d	Minimize $\Sigma(\lambda_i-\beta_i)^2$	$\frac{\lambda_i}{\lambda_{01}}$ i	$\beta_i = 2\lambda_{0i}$ $i \neq 2$
				$\beta_2 = \lambda_{02}$

TABLE 5

Three Frequency Separation Constraints for
Optimization Problem of Table 7 (OPT1a)

		$g_1 = \frac{1}{r_1}\left(\frac{\lambda_2}{\lambda_1}\right) - 1$	$g_2 = \frac{1}{r_2}\left(\frac{\lambda_3}{\lambda_2}\right) - 1$	$g_3 = \frac{\lambda_4}{\lambda_3} - 1.5$
$\Sigma n_i = 12$	*	0.33	0.0	0.00
	**	0.42	-0.08	-0.036
	***	0.30	0.00	0.00
$\Sigma n_i = 18$	*	0.015	0.0	0.00
	**	-0.017	0.09	-0.06
	***	0.00	0.00	0.00
$\Sigma n_I = 24$	*	0.00	0.00	0.00
	**	-0.01	0.019	-0.01
	***	0.00	0.00	0.00

* First Continuous Solution,
** Rounded Off Solution
*** Optimal Solution

TABLE 6

Definition of Frequency Separation Constraints and Target Frequencies

Frequency Separation Constraint Definition for (OPT1b, OPT2a, OPT2b, OPT2c, OPT2d)	Initial Frequencies λ_i	Target Frequencies β_i OPT2a	OPT2b	OPT2c	OPT2d
$\frac{\lambda_1}{\lambda_{01}} > 1.0$	1.0	3.57	3.93	4.29	2.0
$\frac{\lambda_2}{\lambda_{01}} > 3.0$	3.57	9.97	10.97	11.96	3.57
$\frac{\lambda_3}{\lambda_{01}} > 10.0$	9.97	10.38	11.42	12.46	19.94
$\frac{\lambda_4}{\lambda_{01}} > 11.0$	10.38	16.60	18.26	19.92	
$\frac{\lambda_5}{\lambda_{01}} > 18.0$	16.60	22.02	24.23	26.43	
$\frac{\lambda_6}{\lambda_{01}} > 24.0$	22.02	32.48	35.73	38.98	
$\frac{\lambda_7}{\lambda_{01}} > 35.0$	32.48	43.61	47.97	52.33	
$\frac{\lambda_8}{\lambda_{01}} > 47.0$	43.61				

TABLE 7

Optimization Results with Three Frequency Separation Constraints Defined in Table 5 (OPT1a)

Design Variables	$\Sigma n_i = 12$			$\Sigma n_i = 18$			$\Sigma n_i = 24$		
	*	**	***	*	**	***	*	**	***
n_1	4.17	4	4	5.83	6	6	4.62	5	6
n_2	0.00	0	0	2.91	3	2	4.29	4	3
n_3	0.01	0	1	0.22	0	1	2.54	3	3
n_4	0.35	0	0	0.26	0	0	3.29	3	2
n_5	0.92	1	0	0.00	0	0	2.51	3	3
n_6	2.75	3	1	4.28	4	4	3.8	4	6
n_7	3.78	4	6	4.49	4	5	2.89	3	1
a_1	0.60	0.60	0.59	0.00	0.00	0.00	0.00	0.00	0.00
a_2	0.10	0.10	0.10	0.07	0.07	0.26	0.00	0.00	0.00
a_3	0.60	0.60	0.57	0.00	0.00	0.00	0.00	0.00	0.00
a_4	0.10	0.10	0.10	0.00	0.00	0.19	0.00	0.00	0.35
a_5	0.10	0.10	0.10	0.00	0.00	0.00	0.95	0.95	1.00
a_6	0.60	0.60	0.52	0.00	0.00	0.00	0.00	0.00	0.00
a_7	0.40	0.40	0.58	0.00	0.09	0.00	0.00	0.00	0.00
a_8	0.10	0.10	0.10	1.00	1.00	0.85	1.00	1.00	0.97
$\frac{\lambda_1}{\lambda_{01}}$	1.281	1.234	1.237	0.911	0.814	0.90	1.088	1.086	1.090

* First Continuous Solution,
** Rounded Off Solution
*** Optimal Solution

TABLE 8

Optimization Results for Case OPT1b with Seven Frequency Separation Constraints Defined in Tables 6,7

	Initial Design	First Continuous Design	Rounded Off Design	Optimal Design
n_1	2	2.38	2	2
n_2	2	0.716	1	1
n_3	2	0.571	1	1
n_4	2	1.024	1	1
n_5	2	1.847	2	2
n_6	1	2.002	2	1
n_7	1	3.460	3	4
a_1	0.5	0.0	0.0	0.0
a_2	0.5	0.0	0.0	0.0
a_3	0.5	0.0	0.0	0.0
a_4	0.5	0.0	0.0	0.0
a_5	0.5	1.0	1.0	1.0
a_6	0.5	1.0	1.0	1.0
a_7	0.5	1.0	1.0	1.0
a_8	0.5	1.0	1.0	1.0
$\frac{\lambda_1}{\lambda_{01}}$	1.0	3.250	3.23	3.240
Number of Frequency Constraints Violated	7	NONE	NONE	NONE

TABLE 9

Iteration Time History for Optimization Problem OPT1b of Table 6

Subproblem Number	Number of Design Variables	CPU Time in Seconds	% CPU Time $(\frac{T}{T_o}) \times 100$	Integer Feasible
1	15	$558-T_o$	100	No
2	15	81	14	No
3	15	82	14	No
4	14	76	13	No
5	14	75	13	No
6	13	73	13	No
7	12	67	12	No
8	11	61	10	No
9	11	61	10	No
10	10	56	10	Yes
11	15	81	14	No
12	15	82	14	No
13	15	81	14	No
14	15	81	14	No
15	15	81	14	No
16	15	81	14	No
17	15	81	14	No
18	15	80	14	No
19	15	80	14	No
20	14	125	22	No
21	13	25	4	Yes
22	14	50	9	No

TABLE 10

Summary of Structural Optimization Results

	Initial Design Vector	Final Design Vector				
		OPT1b	OPT2a	OPT2b	OPT2c	OPT2d
n_1	2	2	2	2	2	4
n_2	2	1	2	2	2	4
n_3	2	1	2	2	2	0
n_4	2	1	1	1	1	0
n_5	2	2	3	3	1	0
n_6	1	1	1	1	1	0
n_7	1	4	1	1	3	4
a_1	0.5	0.0	0.016	0.0	0.0	0
a_2	0.5	0.0	0.024	0.0	0.0	1.0
a_3	0.5	0.0	0.096	0.046	0.0	0.0
a_4	0.5	0.0	0.329	0.404	0.019	0.0
a_5	0.5	1.0	0.976	1.000	1.00	1.0
a_6	0.5	1.0	0.894	1.000	1.00	0.0
a_7	0.5	1.0	0.992	1.000	1.00	0.137
a_8	0.5	1.0	0.278	0.505	0.981	1.0
$\frac{\lambda_1}{\lambda_{01}}$	1.0	3.25	2.69	2.92	3.18	2.16

TABLE 11

Structural Frequencies for Optimized Structures

	Initial Design	Structural Frequencies for the OPT1b	OPT2a	OPT2b	OPT2c	OPT2d
$\frac{\lambda_1}{\lambda_{01}}$	1.0	3.25	2.69	2.92	3.18	2.16
$\frac{\lambda_2}{\lambda_{01}}$	3.57	11.26	7.86	8.93	10.13	3.58
$\frac{\lambda_3}{\lambda_{01}}$	9.97	13.46	12.00	12.32	13.99	15.46
$\frac{\lambda_4}{\lambda_{01}}$	10.38	24.69	18.06	20.36	23.98	16.6
$\frac{\lambda_5}{\lambda_{01}}$	16.60	32.82	23.07	24.15	26.72	18.9
$\frac{\lambda_5}{\lambda_{01}}$	22.03	43.68	37.58	41.75	42.24	29.0
$\frac{\lambda_7}{\lambda_{01}}$	32.48	52.24	47.15	47.96	47.96	46.2
$\frac{\lambda_8}{\lambda_{01}}$	43.61	61.0	47.47	50.12	55.31	50.0

TABLE 12

Loads Used to Simulate Initial Disturbance

Node Number	Degree of Freedom	Magnitude of Load Applied		
		Load 1	Load 2	Load 3
17	23	1.0	-2.0	-1.0
19	29	2.0	-1.0	-2.0
21	35	1.0	1.0	-2.0
31	57	1.0	-2.0	1.0
33	63	2.0	0.0	0.0
35	69	1.0	2.0	-1.0
45	91	1.0	-1.0	2.0
47	97	2.0	1.0	2.0
49	103	1.0	2.0	1.0

TABLE 13.a

Modal Displacements Due to Applied Load 1 Defined in Table 12

Mode Number	Initial Structure	Modal Displacements for OPT1b	OPT2a	OPT2b	OPT2c	OPT2d
1	57.41	17.60	21.47	19.64	17.95	29.5
2	.144	-0.0	0.0	0.003	-0.006	-0.03
3	.524	-0.0	0.007	-0.007	-0.006	-2.31
4	.026	- .101	-0.188	0.232	-0.04	- .11
5	-.523	.254	-0.123	-0.085	0.304	0.30
6	0.003	.175	.001	0.0	0.008	- .12
7	0.003	0.0	-0.007	0.162	0.168	.01
8	0.226	0.0	0.165	0.001	0.00	0.00

TABLE 13.b

Modal Displacements Due to Applied Load 2 Defined in Table 12

Mode Number	Initial Structure	Modal Displacements for OPT1b	OPT2a	OPT2b	OPT2c	OPT2d
1	.413	0.028	0.025	0.013	0.025	- .18
2	-14.7	5.37	-6.20	-5.68	5.88	-13.9
3	.138	-0.112	-3.03	2.75	0.763	.16
4	- 3.23	0.008	-0.016	-0.008	0.008	- 0.05
5	- 0.010	0.001	0.004	-0.002	0.0	- 0.3
6	0.392	0.0	0.284	0.185	0.054	0.5
7	0.097	0.05	-0.08	0.0	-0.003	- 0.03
8	0.0	-0.009	-0.004	-0.004	-0.023	0.0

TABLE 13.c

Modal Displacements Due to Applied Load 3 Defined in Table 12

Mode Number	Initial Structure	Modal Displacements for OPT1	OPT2a	OPT2b	OPT2c	OPT2d
1	-0.179	0.020	0.02	0.02	0.02	0.47
2	8.44	0.311	4.40	3.63	-0.851	1.81
3	.133	4.59	-4.17	4.19	4.35	0.74
4	-5.17	0.0	-0.010	0.006	0.0	-4.08
5	-0.014	0.0	-0.006	-0.003	0.0	-1.36
6	0.088	0.001	0.244	0.165	0.044	-0.03
7	-0.124	-0.027	0.0	-0.001	0.001	- .29
8	0.0	0.101	-0.001	0.006	0.020	0.0

TABLE 14

Performance Indices for Unoptimized and Optimized Structures

		R = 0.1	R = 1.0	R = 10.
Initial Structure	Load 1	833	1953	6586
	Load 2	169	410	1239
	Load 3	95	233	7046
OPT1b	Load 1	78	183	619
	Load 2	19	47	142
	Load 3	16	40	121
OPT2a	Load 1	116	273	920
	Load 2	30	73	223
	Load 3	26	63	190
OPT2b	Load 1	97	228	771
	Load 2	25	62	189
	Load 3	22	53	161
OPT2c	Load 1	81	191	644
	Load 2	22	54	163
	Load 3	16	39	117
OPT2d	Load 1	227	533	1792
	Load 2	88	212	661
	Load 3	27	67	203

TABLE 15

Ratios of Performance Index of the Unoptimized Structure to that of the Optimized Structure

		R = 0.1	R = 1.0	R = 10.
OPT1b	Load 1	10.6	10.6	10.6
	Load 2	8.6	8.6	8.6
	Load 3	5.7	5.7	5.8
OPT2a	Load 1	7.1	7.1	7.1
	Load 2	5.5	5.5	5.5
	Load 3	3.6	3.6	3.6
OPT2b	Load 1	8.5	8.5	8.5
	Load 2	6.5	6.5	6.5
	Load 3	4.3	4.3	4.3
OPT2c	Load 1	10.2	10.2	10.2
	Load 2	7.5	7.6	7.6
	Load 3	5.8	5.9	5.9
OPT2d	Load 1	3.6	3.6	3.6
	Load 2	1.9	1.9	1.8
	Load 3	3.4	3.4	3.4

TABLE 16

Norm of the Modal Control Forces for Unoptimized and Optimized Structures

		R = 0.1	R = 1.0	R = 10.
Initial Structure	Load 1	133	23	2.8
	Load 2	26	3.6	0.39
	Load 3	16	2.2	0.23
OPT1b	Load 1	40.8	7.29	0.859
	Load 2	9.71	1.35	0.143
	Load 3	7.94	1.06	0.112
OPT2a	Load 1	49.7	8.89	1.04
	Load 2	12.7	1.81	0.193
	Load 3	10.9	1.51	0.161
OPT2b	Load 1	45.5	8.13	0.959
	Load 2	11.6	1.63	0.174
	Load 3	9.8	1.36	0.144
OPT2c	Load 1	41.6	7.43	0.876
	Load 2	10.9	1.54	0.164
	Load 3	7.5	1.01	0.106
OPT2d	Load 1	68	12	1.4
	Load 2	28	4.3	0.47
	Load 3	7.3	0.96	0.10

TABLE 17

Ratio of Norms of the Modal Control Forces for the Unoptimized and Optimized Structure

		R = 0.1	R = 1.0	R = 10.
OPT1b	Load 1	3.2	3.2	3.2
	Load 2	2.7	2.7	2.7
	Load 3	2.1	2.0	2.0
OPT2a	Load 1	2.6	2.6	2.6
	Load 2	2.0	2.0	2.0
	Load 3	1.5	1.4	1.4
OPT2b	Load 1	2.9	2.9	2.9
	Load 2	2.3	2.2	2.2
	Load 3	1.6	1.6	1.6
OPT2c	Load 1	3.1	3.1	3.1
	Load 2	2.4	2.3	2.3
	Load 3	2.1	2.2	2.1
OPT2d	Load 1	1.9	1.9	1.9
	Load 2	0.94	0.8	0.8
	Load 3	2.2	2.3	2.3

TABLE 18

Effect of Actuator Locations on Actuator Forces for a Given Modal Control Vector (OPT2a, R = 1, Load 3)

Modal Control Forces	Case 1 Actuator Locations (Node Number)	Case 1 Actuator Forces	Case 2 Actuator Locations (Node Number)	Case 2 Actuator Forces
-0.0087	16	0.761	17	-1.807
-1.194	17	-0.971	22	-0.373
0.9386	18	0.144	33	-0.294
-0.0019	22	0.831	34	0.128
0.0010	31	-0.128	40	1.134
0.0321	33	0.714	41	0.415
+0.0	36	0.889	46	-0.618
		Norm = 1.88		Norm = 2.31

TABLE 19

Ratio of Actuator Force Norms of the Unoptimized Structure to that of the Optimized Structure (OPT2a) for Cases 1 and 2 Listed in Table 18

		R = 0.1	R = 1.0	R = 10
Case 1	Load 1	1.86	3.28	1.56
	Load 2	1.06	2.66	0.40
	Load 3	0.36	1.31	0.12
Case 2	Load 1	3.33	2.03	3.10
	Load 2	2.14	1.51	3.14
	Load 3	2.28	2.16	0.62

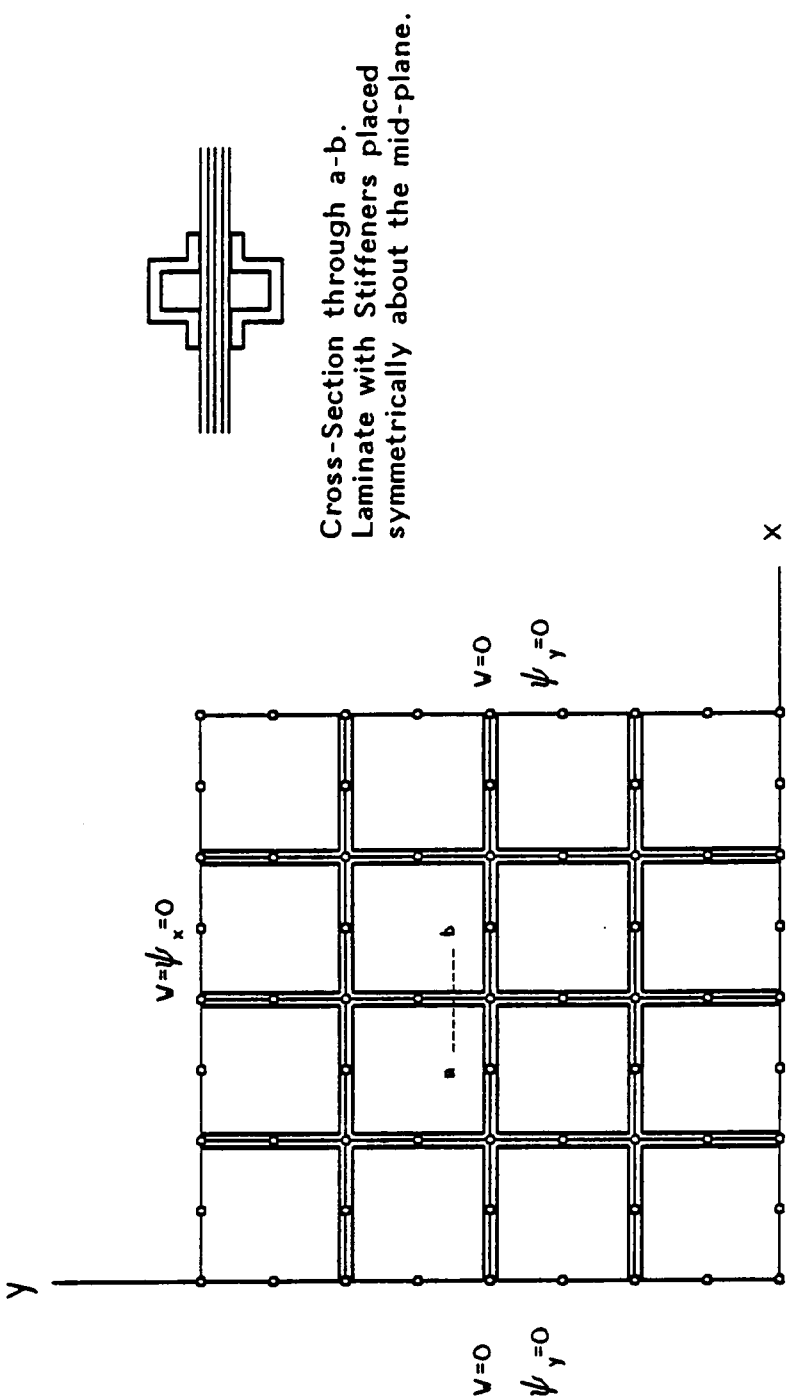

Figure 1. Co-ordinate System, FEM Mesh and Boundary Conditions for the Simply Supported Stiffened Composite Panel.

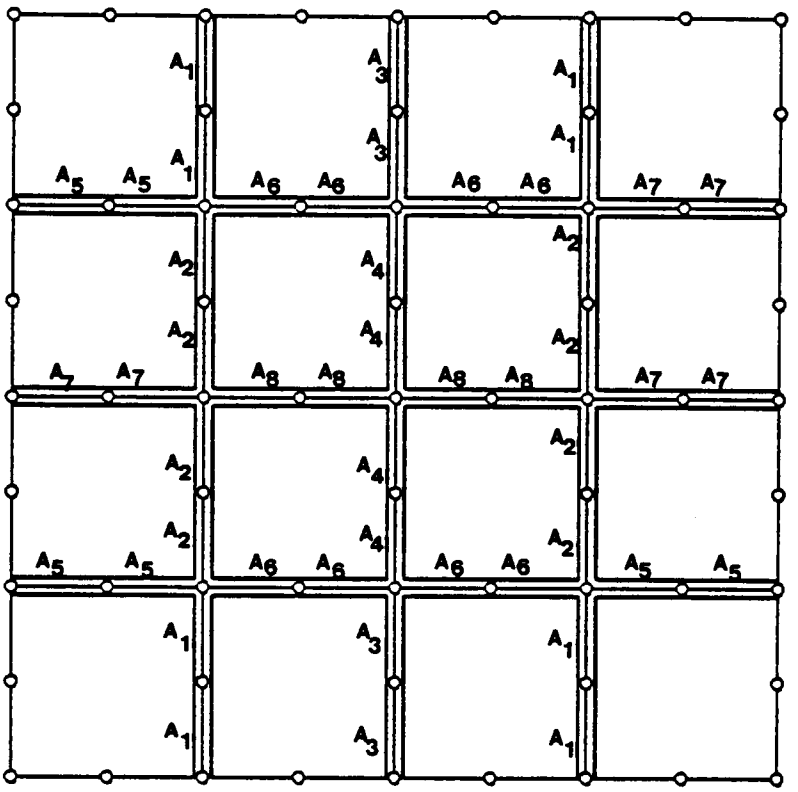

Figure 2. Linking of Design Variables (Stiffener Areas), for the Stiffened Composite Plate.

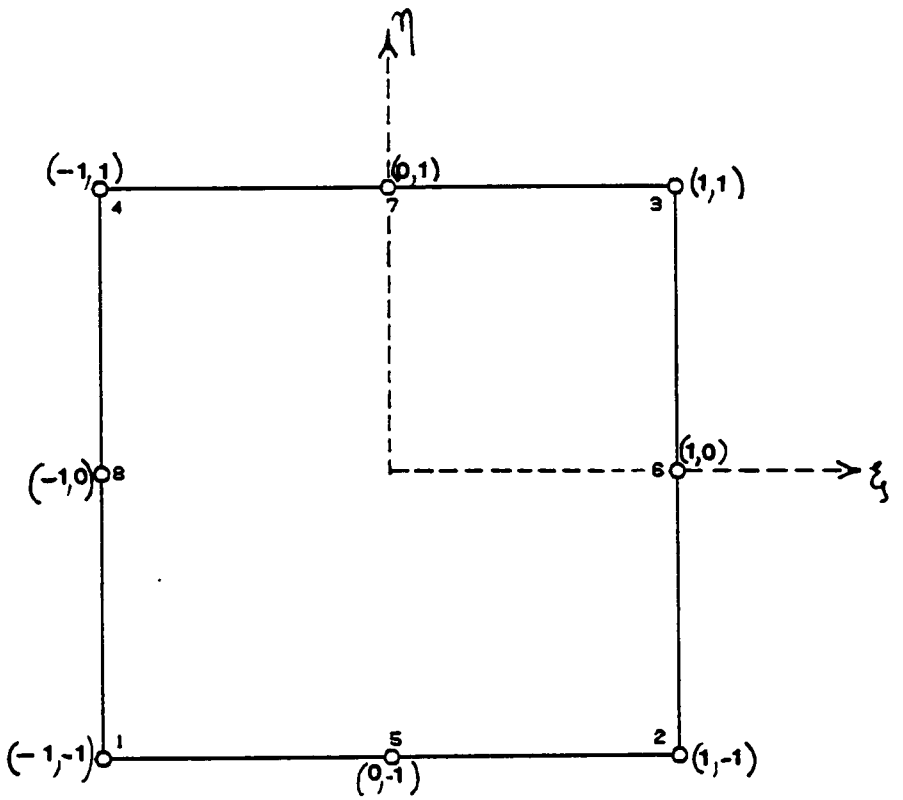

Figure 3. Eight Noded Isoparametric Plate Bending Element with 3 degrees of freedom per node (w, ψ_x, ψ_y)

w Transverse Displacement

ψ_x Shear Rotation about the Y-axis (+ve clockwise)

ψ_y Shear Rotation about the X-axis (+ve clockwise)

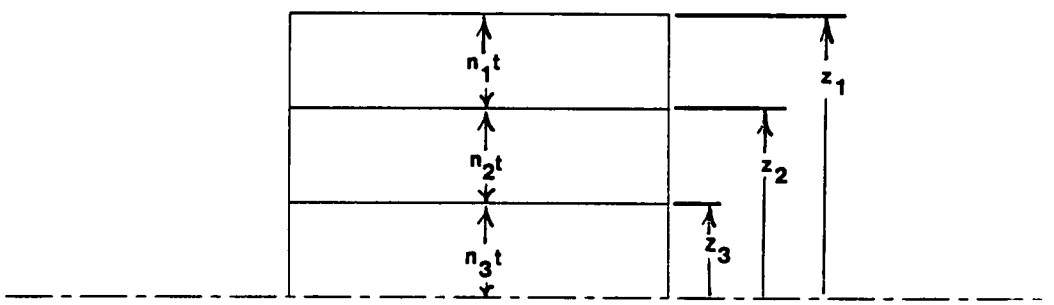

Figure 4. Six ply laminate

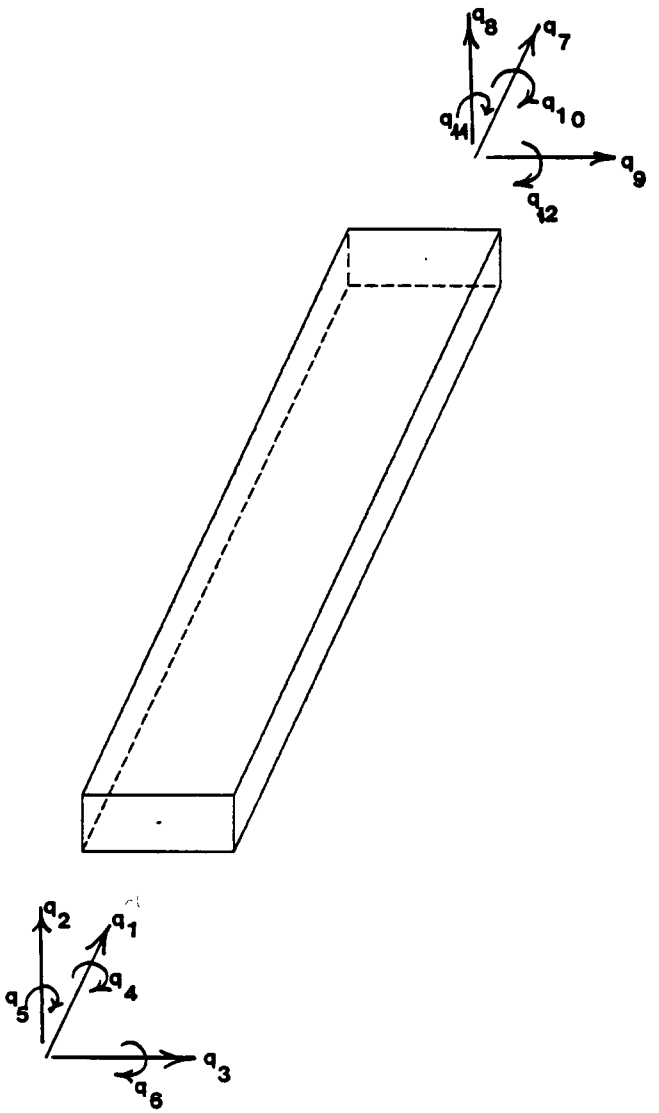

Figure 5. Twelve degree of freedom Frame Element

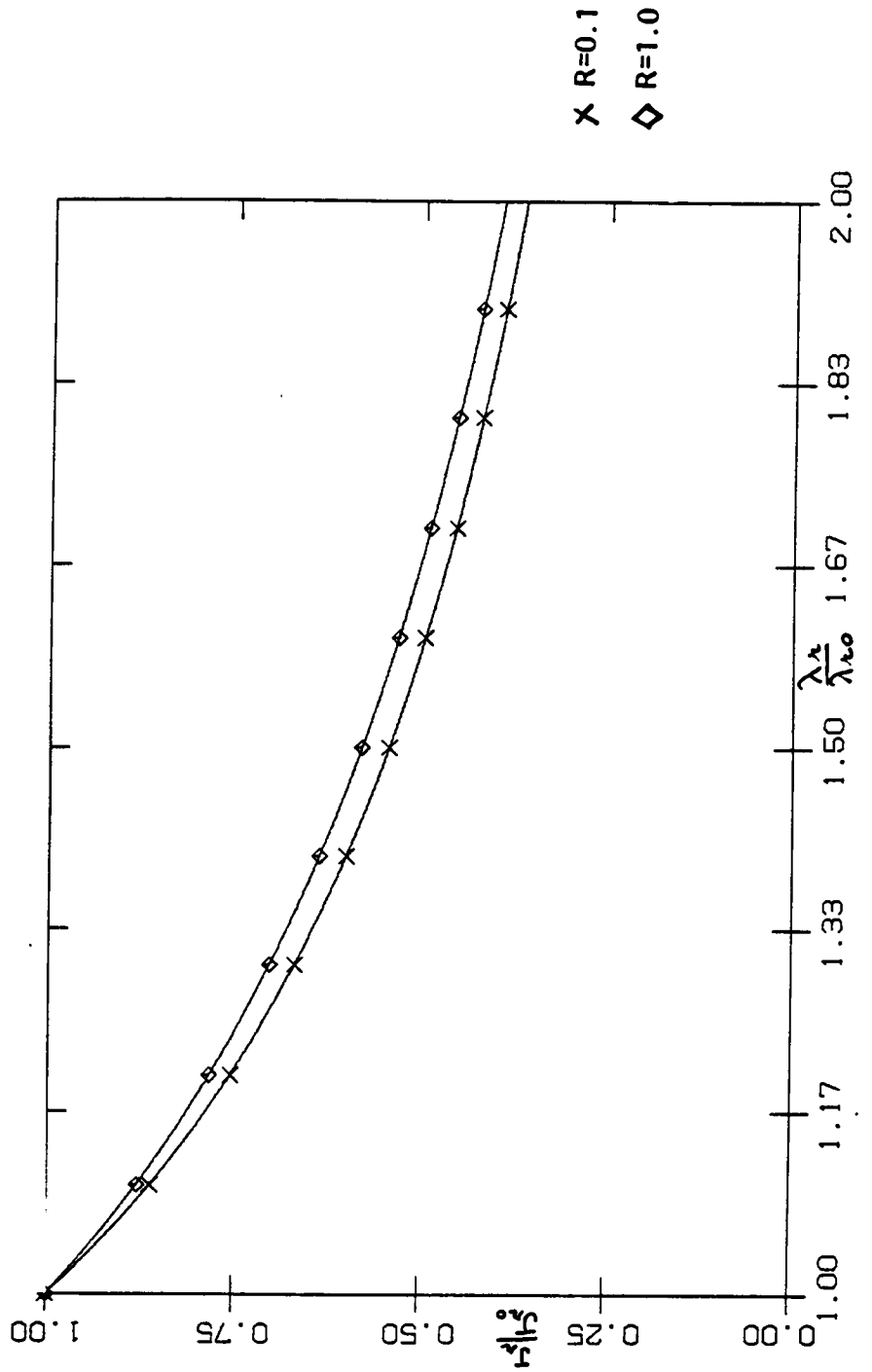

Figure 6. Variation of Performance Index of the 1st mode

The vita has been removed from the scanned document